UNIVERSITÀ POLITECNICA DELLE MARCHE

FACOLTÀ DI **INGEGNERIA**

Corso di Laurea Magistrale **Environmental Engineering**

Geotechnical characterization of dredged sediments in a confined disposal facility

Relatore: Chiar.ma

Prof. **Evelina Fratalocchi**

Tesi di Laurea di:

Martina Gambadori

Correlatore:

Ing. **Federica Pasqualini**

A.A. **2021/2022**

Sommario

I. INTRODUCTION

Silting of the seabed is a typical issue in port basins and involves the need for dredging of significant amounts of marine sediment, often affected by contamination. Among the options provided by the current regulations for the management of dredged sediment (Ministerial Decree No. 173 - 2016), the filling of a Confined Disposal Facility is a sustainable solution provided that the new filled areas can be used as a reclaimed land. This solution requires the improvement of the mechanical characteristics of the disposed sediments, which are typically very poor.

The Port System Authority of the Central Adriatic Sea (Ancona), has deliberated the building of a Confined Disposal Facility (CDF) in the Port's Commercial Dock, combining the need for dredging sediments to maintain the accessibility of the port's docks with the need to expand cargo storage spaces. Specifically, in 2015 a CDF of about 9.5 ha was built. The area was divided into sectors as sediments would be disposed at different times.

The consolidation of each sector can be carried out at the end of its filling, and in this way, it will be possible to reduce the time of the completion work, being able to manage in parallel the consolidation process of the filled sector and the conferment of sediments in other sectors.

To date, the filling of the first sector has been completed, and the consolidation of that area has already been carried out in an area used as a test-field.

The present thesis focuses on the geotechnical characterization of the sediments in the first sector. Specifically, after the consolidation phase, boreholes with undisturbed sampling and cone penetration tests (CPT) were carried out, that allowed to identify homogeneous stratigraphic units. Based on the results obtained after the consolidation phase and considering the data obtained from the CPTs, on the basis of literature, an empirical site-specific correlation was determined between the undrained shear strength of the sediments and the cone resistance.

The first part of the thesis, after description of the site, discusses the methodology used throughout, describing the various tests and reference standards.

In the second part all the results obtained are illustrated and discussed.

II. THE CONFINED DISPOSAL FACILITY (CDF) OF ANCONA'S PORT

A confined disposal facility (CDF) was built at the Ancona Harbour (Italy), located in the commercial dock, to host contaminated dredged sediments. Its internal area (9.5 ha) includes sediments disposed soon after its construction, emerging 1 m above the sea level. The current mean water depth in the remaining part (4.5 ha) is 4 m, with a maximum of about 7 m. The CDF was built by steel sheet piling, 20 m long, through a 6 m thick dense sandy layer to the underlying clayey layer (> 12 m), that performs as the natural impervious base. The sheet pile interlocks were sealed by water expanding epoxy resin, in order to ensure the required water tightness (Italian Law L.84/1994), that is, a hydraulic conductivity, $k \leq 1\text{x}10^{-9}$ m/s.

FIGURE 1 ANCONA'S HARBOUR

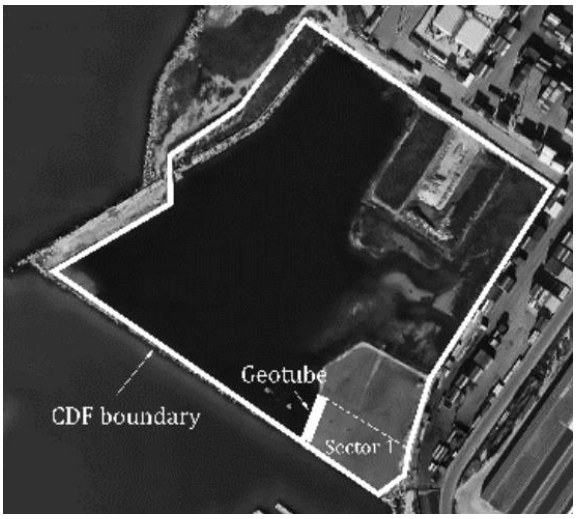

FIGURE 2 CDF IN ANCONA'S PORT AND FIRST SECTOR FILLED WITH DREDGED MATERIAL

The scheduling of sediments disposal had to take into account that the disposal would be staggered over several months or years, and for this reason a partition in sectors of the CDF was planned, in order to manage the filling steps and the subsequent sediment consolidation. (Felici et al., 2019).

The first sector was created in adjacency to one of the CDF walls, using special geotextile bags (geo-tubes) filled with the sediments themselves (Fig. 3). These geo-tubes avoid the loss of the CDF capacity; they create an effective sidewall confinement for the subsequent consolidation process. This sector, more or less rectangular (50 m x 70 m), is confined at the open side by the geo-tubes, at another side by the piling, and on the remaining two sides it is bordered by land and by the previously disposed sediments.

FIGURE 3 GEOTEXTILE GEOTUBE

The first sector has been completed, and, considering the fine-grained nature of the sediments, the consolidation by preloading combined with vertical drains was selected.

The sediments in the first sector were dredged from 3 different sites: Fano Harbour, Isa-Palumbo and Fincantieri areas, both in the Ancona Harbour.

To evaluate the expected consolidation time and settlements, several samples of the dredged sediments were analysed. The results of their characterization and classification tests are reported in Table 1. In general, the "Fincantieri" and "Fano" sediments can be identified as fine-grained sediments characterized by a medium plasticity, while the "Isa-Palumbo" sediments can be identified as silty sand.

TABLE 1 CHARACTERISTIC OF THE SEDIMENTS IN THE FIRST SECTOR OF THE CDF

	Fincantieri	Fano	Isa-Palumbo
Gravel (%)	1-2	0-1	8-15
Sand (%)	6-7	0-3	51-59
Silt (%)	55-57	60-66	15-20
Clay (%)	36-38	30-35	5-11
Liquid limit (%)	44-50	53-58	20-26
Plasticity index (%)	18-22	25-28	n.p.*
USCS	ML-CL	MH	SM
Organic content (%)	4	6	0
Specific gravity (-)	2.67	2.72	2.61

*non-plastic

ML: silt; CL: clay of low plasticity; MH: silt of high plasticity; SM: silty sand.

Incremental load oedometer tests (ASTM D2435) on reconstituted samples (high void ratios), saturated with sea water, were carried out to study the sediment compressibility and consolidation. The applied effective vertical pressures (σ'_v) ranged from 6.25 kPa to 400 kPa.

The mean values of the parameters relevant to the design pressure range are listed in Table 2 for each of the sediments (c_v = vertical consolidation coefficient; c_c = compression index; E_{oed} = oedometric modulus). The vertical hydraulic conductivity values, k_v, determined from the oedometer tests by the Terzaghi one-dimensional consolidation theory, were compared with those measured by consolidometer tests (ASTM D5856), in order to evaluate their reliability and possible use to design the consolidation technique without *k* testing. It is worth highlighting that for void ratios, *e*, ranging from 1.3 to 2.0, a good agreement between the results of the two tests was found for the "Fincantieri" sediments, with k_v values from 4×10^{-10} m/s to 1×10^{-9} m/s, increasing with *e* (Felici et al., 2022).

TABLE 2 PARAMETERS FROM INCREMENTAL LOAD OEDOMETRIC TEST

σ'_v (kPa)	E_{oed} (MPa)	e (-)	c_v (m²/s)	k_v (m/s)	c_c (-)
"Fincantieri"					
12.5	0.22	1.89	2.4×10^{-8}	3.1×10^{-9}	0.68
25	0.58	1.81	4.4×10^{-8}	1.0×10^{-9}	0.29
50	0.68	1.64	3.1×10^{-8}	5.1×10^{-10}	0.57
100	1.62	1.52	3.9×10^{-8}	2.9×10^{-10}	0.44
"Fano"					
12.5	0.20	1.60	1.7×10^{-8}	1.0×10^{-9}	0.23
25	0.26	1.50	1.6×10^{-8}	6.9×10^{-9}	0.34
50	0.40	1.36	1.8×10^{-8}	5.5×10^{-10}	0.46
100	0.87	1.23	2.3×10^{-8}	3.2×10^{-10}	0.43
"Isa-Palumbo"					
12.5	0.59	0.77	2.1×10^{-8}	4.8×10^{-10}	0.15
25	1.11	0.71	1.8×10^{-7}	5.8×10^{-10}	0.11
50	3.06	0.71	9.6×10^{-8}	3.3×10^{-10}	0.13
100	2.99	0.67	1.4×10^{-7}	3.8×10^{-10}	0.14

After the characterization of the sediments disposed in this sector, the site investigation was performed with 6 piezocone tests (CPTUs) and 8 mechanical cone penetration tests (CPTs). The CPT_S were distributed across the future footprint of the embankment (Fig. 4) to investigate the sediment mechanical characteristics and stratigraphy, while CPTUs, being a more reliable and accurate tool, were located in the central area.

The same tests have been performed also after the consolidation phase, more or less in the same locations of the previous ones.

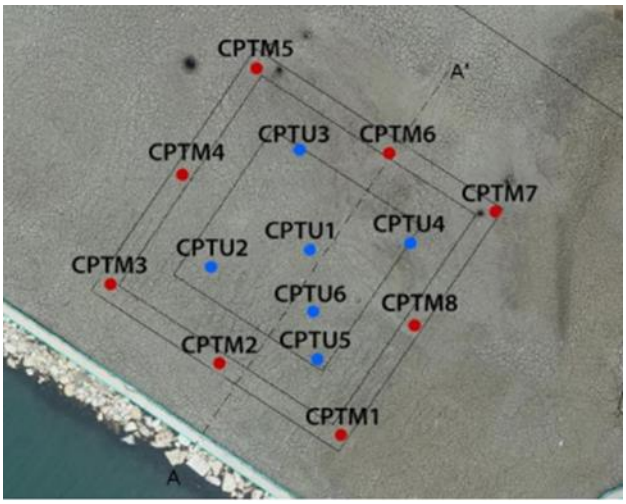

FIGURE 4 IN-SITU SOIL INVESTIGATION (CPTM AND CPTU)

The consolidation of the first sector was carried out with the so called "moving bank" method (Pasqualini et al., 2014*):* the same material used for the preloading embankment, will be reused

to consolidate the sediments in the other sectors. The improvement technique by preloading and vertical drains was selected, to achieve consolidation settlements in the time of few months.
First, a layer of coarse material (about 0.7 m thick) has been placed above the sediments to allow the vehicles to operate and also to act as top drainage for the vertical drains (the bottom drainage for the sediment layer is the underlying natural sandy layer). After this, prefabricated vertical drains (PVDs) were installed: the selected product is Colbonddrain (Fig. 5)**,** made by a polyethylene core on which a needle-punched polypropylene geotextile filter is pasted. Their section is characterized by a width of 10 cm and a thickness of 0.5 cm.

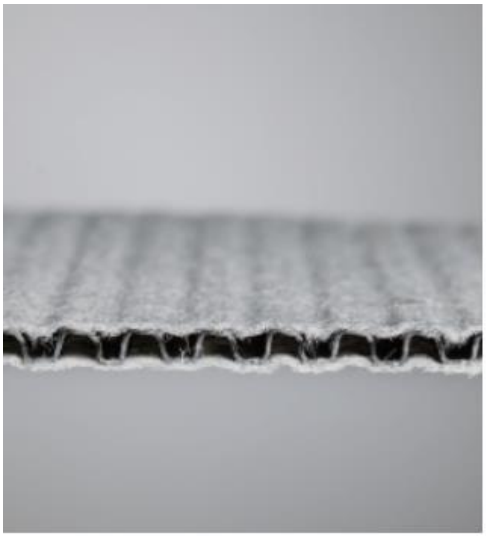

FIGURE 5 COLBONDDRAIN PVD

At the end, the preloading embankment was built with coarse material available on site (boulders residuals and construction rubbles), thus preventing the exploiting of quarries.
The embankment was built on a square area of 30 m side with a slope of 45°, and in order to prevent instability, it was gradually built.

Fig. 6 shows a schematic section of the test field.

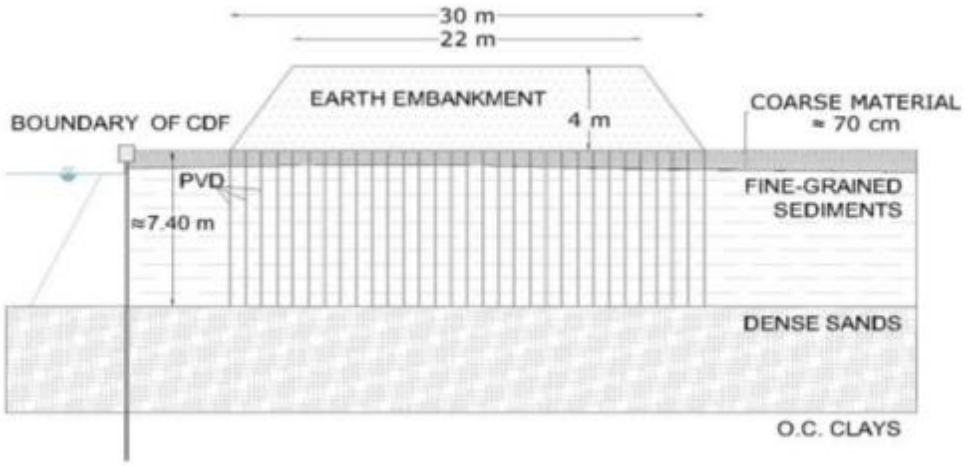

FIGURE 6 SCHEMATIC CROSS SECTION OF THE TEST FIELD

Before the construction of the embankment, some monitoring instruments have been installed. In particular, the monitoring of test field has been performed using 2 pressure cells to measure (C1 and C2), 5 drive-in piezometers to measure the water interstitial pressure (P1, P2, …) and 10 settlement gauges (A1, …, A10), as shown in Fig. 7. These instruments were used to measure the stress applied by the embankment, the pore pressure in the sediment layer and the settlements during the entire consolidation phase, respectively. The results of monitoring have confirmed the design assumptions, in particular the end of the consolidation process in a few months after loading.

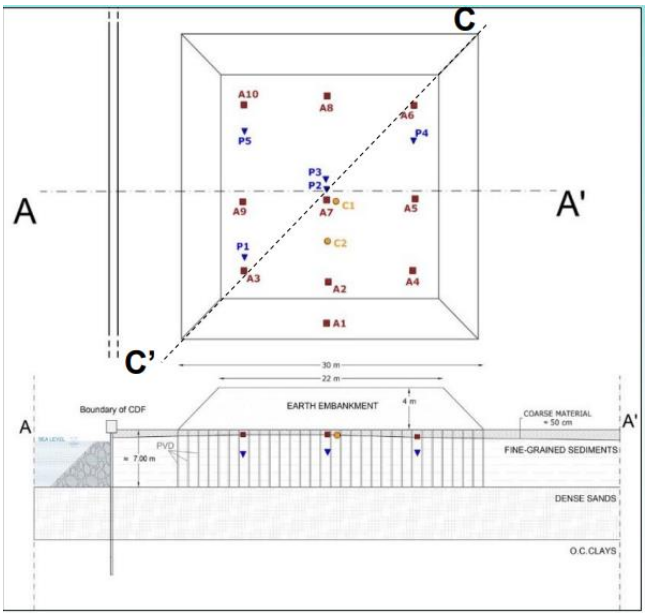

FIGURE 7 PLACEMENT OF PRESSURE CELLS, PIEZOMETERS AND SETTLEMENT GAUGES

III. METODOLOGY

2.1 CPT

Among the many devices that can be used in situ, the static electric or mechanic penetrometers are the most versatile instruments for soil investigation.

Electric cone penetration tests (CPT) have undergone great development in the recent decades, and in particular the use of those with pore pressure measurements (CPTu) is increasingly used in professional practice. One of the major applications of the CPT is for stratigraphic profiling along a vertical. One of the most important characteristics of this test is the repetitiveness of the measurements, which allows for continuous recordings of the cone penetration resistance (q_c), and sleeve friction (fs).

A typical system for the execution of a CPT test includes: (1) a mechanic penetrometer or a piezocone, (2) a hydraulic thrust system, (3) a transmission system, (4) a depth gauge, (5) a data acquisition unit.

The test is self-piercing, i.e., it does not require a borehole to be drilled, and consists of the pressurized insertion into the soil, from ground level and at a constant speed of 20 mm/sec (with a tolerance of ±5 mm/sec), of a conical bit having a diameter of 35.7 mm and an opening angle of 60°, connected to the pushing device by a battery of pipes. The contrast necessary to insert the penetrometer is usually obtained with the weight of the truck, possibly ballasted, on which the equipment is installed.

The measurement of cone penetration resistance (q_c) and sleeve friction (fs) are performed locally and independently of each other with electrical transducers, that send signals to the control unit (located on the surface). The data are directly acquired in numerical form and even graphed during the test execution.

The upgrade of this type of test is the CPTu, that is the same device, but it is equipped with a porous ceramic or steel element, placed at the base of the conical tip, that allows to measure and record the pore pressure (u) both during the piezocone activity and while the piezocone is stationary.

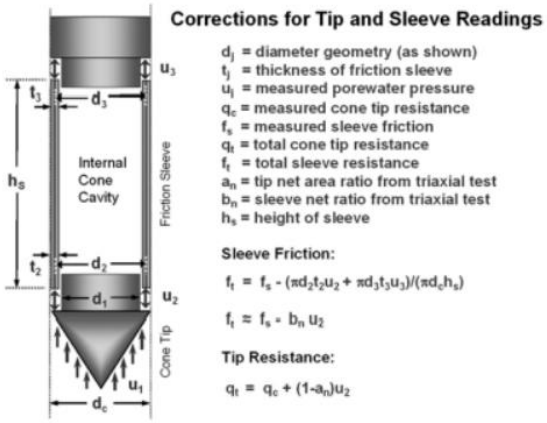

FIGURE 8 SCHEMATIC VIEW OF THE CPTU PROBE

2.2. CPTU results interpretation

The CPTu (and CPT) tests have three main applications: the determination of the soil stratigraphy and the identification of the different soils, the estimation of geotechnical parameters, and the direct employment in design works.

The measured strength for the insertion of the conical bit (Q_c) divided by the bit base area (A_c) gives the measured bit resistance, $q_c=Q_c/A_c$.

For the interpretation of the test results, it is necessary to evaluate the corrected total cone resistance (q_t) taking into account the so called "unequal end area effects", according to which the interstitial pressure acts on unequal areas. Baligh et al. (1981) and Campanella et al. (1982) proposed the following correction:

$$q_t = q_c + (1 + a)u \qquad [1]$$

where u is the pore pressure measured between the cone tip and the friction sleeve and a is the net area ratio. Typically, the net area ratio is given by:

$$a \approx \frac{d^2}{D^2} \qquad [2]$$

where d is the diameter of load cell support and D is the diameter of the cone. In general, many cone penetrometers have values of cone area ratios between 0.9 and 0.55, but sometimes this ratio can assume values lower than 0.38: an a value lower than 0.38 should be considered unacceptable when CPT tests are performed in very soft fined-grained soils, because the correction becomes the major contribution to q_t with potential increased loss of accuracy.

A similar correction can be applied to the sleeve friction as proposed by Lunne et al. (1986) and Konrad (1987). The total stress sleeve friction f_t will be:

$$f_t = f_s - \frac{(u_2 * A_{sb} - u_3 * A_{st})}{A_s} \qquad [3]$$

where, u_3 is the pore pressure at the upper end of the sleeve, u_2 is the pore pressure at the low end of the sleeve, A_{st} is the area of friction sleeve at top, A_{sb} is end area of friction sleeve at bottom, and A_s is outside surface area of friction sleeve.

Commonly, this correction is not applied, because during the CPTu test only the u_2 pressure is measured.

What must be accounted is the influence of the soil unit weight and groundwater conditions: for this reason, Wroth (1984) suggested that CPT data should be normalized using the following parameters:

1. Normalized cone resistance: $Q_{tl} = \frac{q_t - \sigma_{vo}}{\sigma'_{vo}}$ [4]
2. Normalized friction ratio: $F_r = \frac{f_s}{q_t - \sigma_{vo}} * 100\%$ [5]
3. Pore pressure ratio: $B_q = \frac{\Delta u}{q_t - \sigma_{vo}}$ [6]

where σ'_{vo} is the in situ effective vertical stress, σ_{vo} is the in situ total vertical stress, Δu (Δu=u_2-u_0) is the excess penetration pore pressure.

The use of these normalized parameters allows the definition of the soil behaviour type (SBT) thanks to the classification charts proposed by Robertson.

2.2.1 Soil behaviour type (SBT)

The most common soil classification system based on the results of cone penetration test is represented by the soil behaviour type charts.. It is necessary to take into account that the SBT chart defines the mechanical behaviour of the soil, and it does not directly provide a classification of the soil based on grain size and plasticity such as the USCS. Typically, soil classification criteria based on grain-size distribution and plasticity often relate reasonably well

to in situ soil behaviour and hence, there is often a good agreement between USCS-based classification and CPT-based SBT.

The definition of the SBT of a soil can be done following two different methodologies: one is based on corrected parameter obtained by CPTUs, the other is based on normalized parameters. Following the corrected parameters methodology, Robertson (1986) proposed two different classification charts: one based on q_t and R_f, and another one based on q_t and B_q, where q_t is the corrected cone resistance (eq. [1]), B_q is the pore pressure ratio (eq. [6]) and R_f is the friction ratio, evaluated with the following equation:

$$R_f = \frac{f_s}{q_c} * 100\% \qquad [7]$$

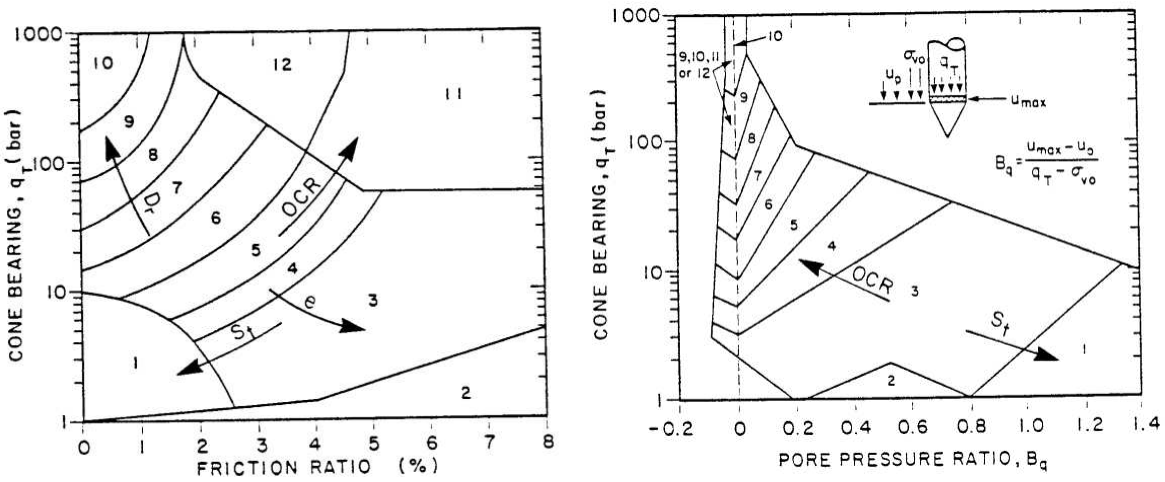

FIGURE 9 SBT CLASSIFICATION CHART BY ROBERTSON (1986)

In the SBT charts of Fig.9, 12 soil types are identified:

1. Sensitive fine grained
2. Organic material
3. Clay
4. Silty clay to clay
5. Clayey silt to silty clay

6. Sandy silt to clayey silt
7. Silty sand to sandy silt
8. Sand to silty sand
9. Sand
10. Gravelly sand to sand
11. Very stiff fine grained (overconsolidated or cemented)
12. Sand to clayey sand (overconsolidated or cemented)

A particular aspect of the charts is that they can be equally well used with uncorrected or corrected cone resistance, since the difference between q_c and q_t is small, except in soft fine-grained soils that produce high penetration pore pressure (Robertson, 2010).
Robertson (2010) proposed an update of the SBT charts: he reduced the number of zones from 12 to 9, in order to match the Robertson (1990) chart; reducing the number of SBT zones an easier comparison between the normalized and non-normalized SBT charts is achieved.
Table 3 summarizes the unification of the 12 zones:

TABLE 3 UNIFICATION BETWEEN 12 SBT ZONES (ROBERTSON, 1986) AND 9 SBTN ZONES (ROBERTSON, 1990)

SBT zone *Robertson et al (1986)*	SBT_n zone *Robertson (1990)*	Proposed common SBT description
1	1	*Sensitive fine-grained*
2	2	*Clay - organic soil*
3	3	*Clays: clay to silty clay*
4 & 5	4	*Silt mixtures: clayey silt & silty clay*
6 & 7	5	*Sand mixtures: silty sand to sandy silt*
8	6	*Sands: clean sands to silty sands*
9 & 10	7	*Dense sand to gravelly sand*
12	8	*Stiff sand to clayey sand**
11	9	*Stiff fine-grained**

** Overconsolidated or cemented*

Dealing with the SBT charts following the normalized parameters, Robertson (1990) proposed a new SBT chart (SBTn) using the normalized and dimensionless cone parameters (eq. [4],[5],[6]). Also in this case, he suggested two different charts based on either Q_{tl}-F_r or Q_{tl}-B_q, as shown in Fig. 10.

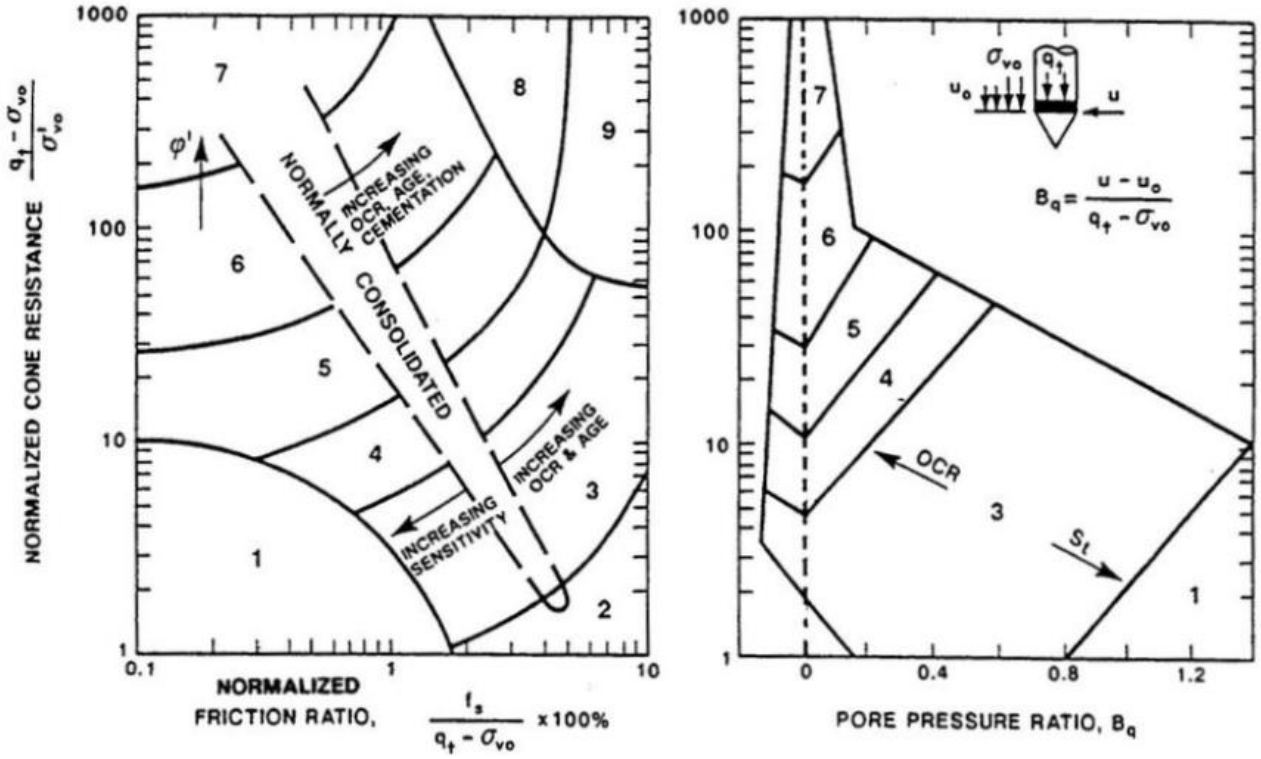

FIGURE 10 ROBERTSON SBT CLASSIFICATION CHARTS (1990)

In the Q_{tl}-F_r classification charts nine different soil behaviour types can be identified:

1. sensitive fine-grained soils
2. organic soils and peat
3. clays (clays to silty clays)
4. silty mixtures (clayey silt to silty clay)
5. sand mixtures (silty sand to sandy silt)
6. sand (clean sand to silty sand)
7. gravelly sand to sand
8. very stiff sand to clayey sand (heavily overconsolidated or cemented)
9. very stiff, fine grained (heavily overconsolidated or cemented)

Included in the SBTn classification charts there is a zone that represents approximately the normally consolidated soil behaviour. Typically, soils that fall in zones 6 and 7 represent approximately drained penetration, while soils in zones 1, 2, 3, and 4 represent undrained penetration. Soils in zones 5, 8 and 9 may represent partially drained penetration.

Several parameters such as changes in stress history, in situ stresses, sensitivity, stiffness, microfabric, and void ratio will influence the classification, and occasionally soils will fall within different zones in each chart; in this case judgement of the pore pressure rate of dissipation is required to correctly classify the soil (Robertson, 1990).

Jefferies and Davies (1993) identified a soil behaviour type index I_c, could represent the SBTn zones in the Q_{tl}-F_r chart. I_c is essentially the radius of concentric circles that define the boundaries of soil types.

As part of liquefaction studies, Robertson and Wride (1998) modified the definition of I_c to apply it to the Robertson (1990) Q_{tl}-F_r chart:

$$I_C = [(3.47 - logQ_{tl})^2 + (logF_r + 1.22)^2]^{0.5} \qquad [8]$$

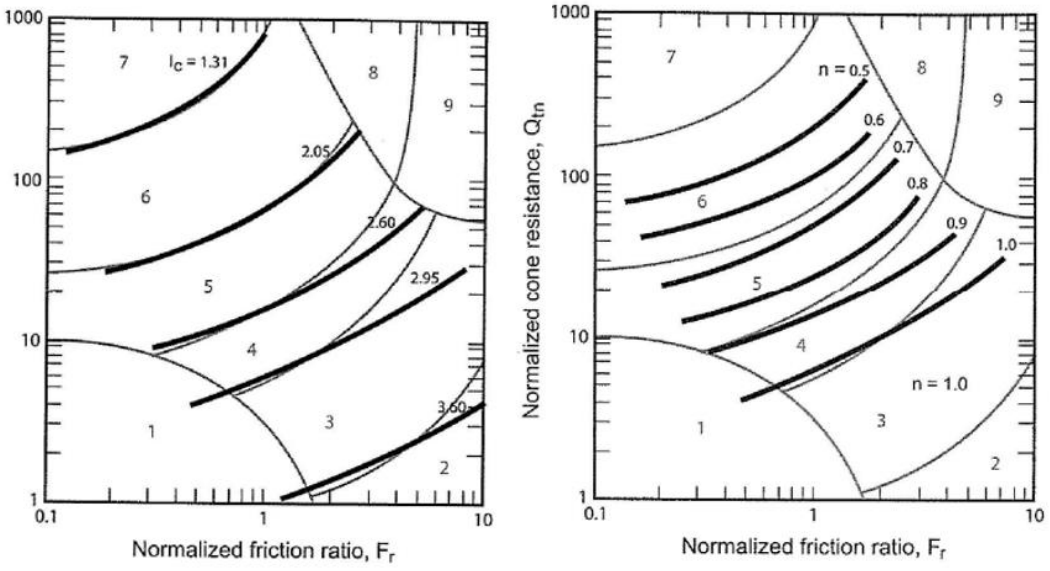

FIGURE 11 (A) CONTOURS OF SBT INDEX (IC) ON SBTN AND (B) CONTOURS OF STRESS EXPONENT N ON SBTN

Eq. [8] and the contours of I_c in Fig. 11A show that I_c is not overly affected by the potential lack of accuracy in the measurement of sleeve friction f_s, but is more dependent on the tip resistance q_t. In using equation [8], if f_s varies by ±50%, the resulting variation in I_c is generally less than ±10%. For soft soils that fall within the lower part of the Q_{tl}-F_r chart, I_c is insensitive to f_s.

Robertson and Wride (1998) and the update by Zhang et al. (2002) suggested a normalized cone parameter with a variable stress exponent n, where:

$$Q_{tn} = [(q_t - \sigma_{vo})/p_a]\,(p_a/\sigma'_{v0})^n \qquad [9]$$

where $(q_t - \sigma_{vo})/p_a$ is the dimensionless net cone resistance, $(p_a/\sigma'_{v0})^n$ is the stress normalization factor, p_a is the atmospheric pressure (same unit as q_t and σ_{vo}), and n is the stress exponent that varies with SBTn. It must be noticed that if n=1, $Q_{tn} = Q_{tl}$. Typical values for n are ≈0.5 in the clean sand region and n≈1 in the clay region, as suggested by several studies (Robertson, 2009).

Robertson (2009) suggested to use the following equation, when n≤1:

$$n = 0.381(I_C) + 0.05(\sigma'_{vo}/p_a) - 0.15 \qquad [10]$$

This relation, as shown in Fig.11B, points out that for most fine-grained soils, the stress exponent will be 1. The stress exponent will range from 0.5 to 0.9 for most coarse-grained soils when in situ vertical stresses are not high; when the in situ vertical effective stress is greater than 1 MPa, the stress exponent is equal to 1 for most soils.

The last update of the SBTn chart by Robertson (2016) considers the property of dilatancy of a soil, that is, the tendency of a soil to increase its volume while shearing. What he noticed is that the SBTn chart of 2009 works well in ideal soils (soils with little or no microstructure that are predominantly young and uncemented), but it can be less effective with structured soils (soils with extensive microstructure, such as caused by aging and cementation). For this reason, the update is focused on the modification of the description of "soil types" by using terms based more on soil behaviour.

Schneider and Moss (2011) established a method to identify sandy soils with microstructure using an empirical parameter K_G:

$$K_G = (G_o/q_t)(Q_{tn})^{0.75} \qquad [11]$$

where G_o is the small-strain shear modulus (=ρ$(V_s)^2$); V_s is the shear wave velocity; ρ is the soil density (=γ/g).

The ratio G_o/q_t was identified as the small-strain rigidity index (I_G), and Robertson suggested that K_G is essentially a normalized rigidity index, since it normalizes the small-strain rigidity index with the in-situ soil state (reflected by Q_{tn}). The I_G index can be extended to include fine-grained soils and it should be defined based on the net cone resistance, since it is a more corrected measure of the soil strength:

$$I_G = G_o/q_n \qquad [12]$$

where q_n=q_t-σ_v.

Hence, the modified normalized small-strain rigidity index, K_G^* is defined:

$$K_G^* = (G_o/q_n)(Q_{tn})^{0.75} \qquad [13]$$

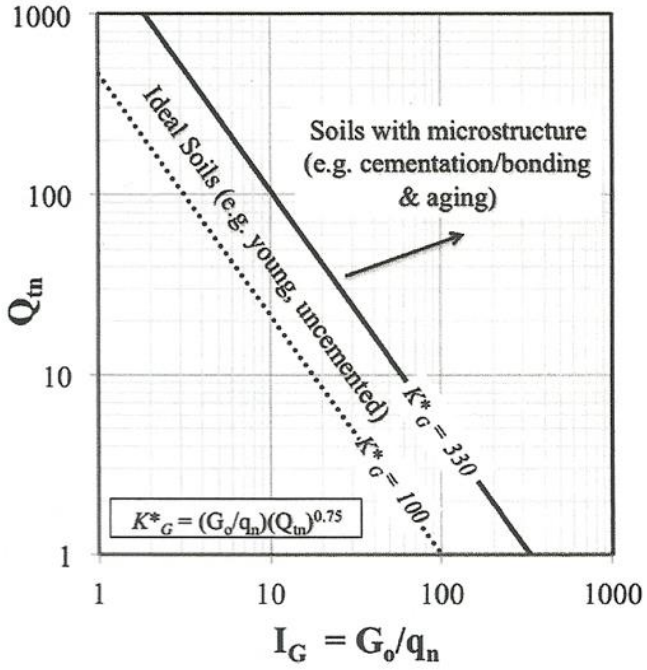

FIGURE 12 QTN-IG CHART TO IDENTIFY THE MICROSTRUCTURE

In general, soils characterized by K_G^* <330 are likely young and uncemented (i.e., they have little or no microstructure) and can be classified as ideal soils; soils characterized by K_G^*>330 tend to have significant microstructure, and they can be classified as structured soils.

Two criteria were used to define the updated SBTn chart: the first is that the contour for the state parameter φ< -0.05 can be used to separate coarse grained ideal soils that can be either contractive or dilative at large strains; the second is that most fine-grained ideal soils with an OCR>4 should have Q_{tn}>12 and are predominantly dilative at large shear strain.

Following these hypotheses, it is possible to develop a simple Q_{tn}-F_r based on boundaries that would separate ideal soils that are either contractive or dilative at large shear strains, by the solid line CD=70. The contractive-dilative (CD) boundary can be represented by the following expression:

$$CD = 70 = (Q_{tn} - 11)(1 + 0.06F_r)^{17} \qquad [14]$$

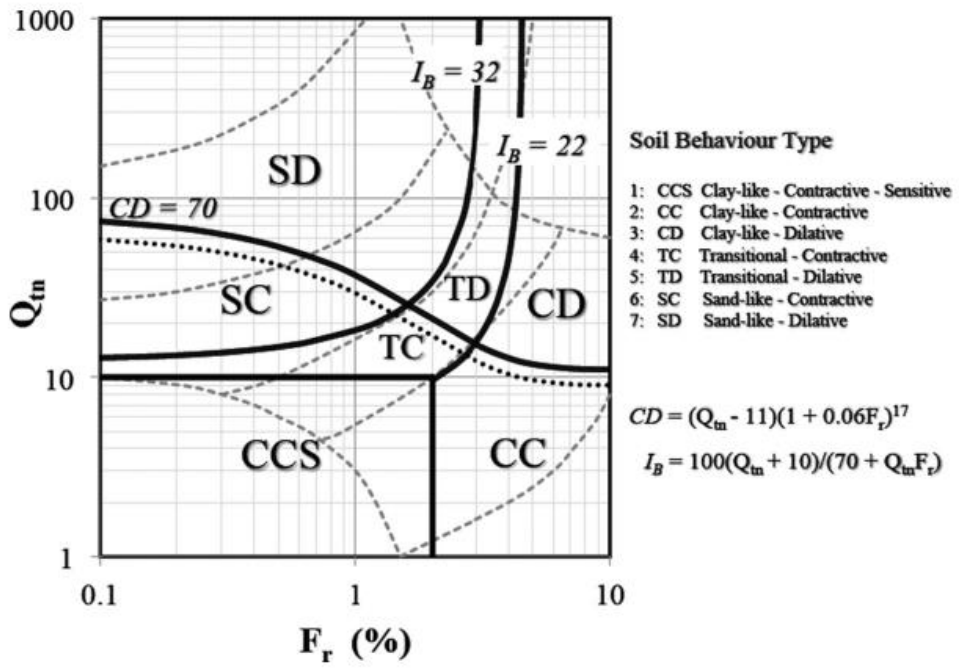

FIGURE 13 UPDATED SBTN CHART BASED ON QTN-FR

when CD>70 the soils are likely dilative at large shear strain.

The dashed line in the chart of Figure 13 shows the lower limit for ideal soils that are predominantly dilative at large shear strain, and it can be represented with the following expression:

$$CD = 60 = (Q_{tn} - 9.5)(1 + 0.06F_r)^{17} \qquad [15]$$

However, Robertson recommended to consider the upper boundary for general geotechnical interpretation, since it is often slightly conservative.

The modified soil behaviour type index (I_B) was introduced by Schneider et al. to obtain a more hyperbolic shape (in terms of $logQ_t$ and $logF_r$) to better capture the SBT boundaries, and it is expressed in the following way:

$$I_B = 100(Q_{tn} + 10)/(Q_{tn}F_r + 70) \qquad [16]$$

- The boundary defined by I_B=32 represents the lower boundary for most sand-like ideal soils and it is similar to the original boundary between SBTn zones 4 and 5 for normally consolidated soils.
- The boundary defined by I_B=22 represents the upper boundary for most claylike ideal soils, and it is similar to the original boundary between SBTn zones 3 and 4 for normally

consolidated soils. Also, the value I_B =22 represents an approximate boundary for plasticity index *PI*~18% in fine-grained ideal soils.

- The region defined for 22< I_B <32 is called "transitional soil", in which soils can have behaviour somewhere between that of either sand-like or claylike ideal soils.

A different approach for soil classification from cone penetration tests was proposed by Eslami and Fellenius (1997). They developed a soil profiling method when investigating the use of cone penetrometer data in pile designs. A database has been compiled consisting of CPT and CPTu data associated with the results of boring, sampling, testing and routine soil characteristics of case from 18 sources reporting data from 20 sites in 5 countries.
They plotted these results considering the effective cone resistance defined as follow:

$$q_E = q_t - u_2 \qquad [17]$$

where q_t is the cone resistance corrected for pore water pressure on shoulder and u_2 is the pore pressure measured at cone shoulder.

They obtained a classification chart, where 5 main soil type categories can be identified:

1. sensitive and collapsible clay and/or silt
2. clay and/or silt
3. silty clay and/or clayey silt
4. sandy silt and/or silty sand
5. sand and/or sandy gravel

In general, the results obtained with the Robertson's chart and the Eslami and Fellenius's charts are similar. The main difference, and advantage of the Eslami and Fellenius soil profiling method is that normalization is not accounted for, hence the input of total and effective stresses in the soil is not required. Also, it avoids the incongruity of plotting data against their own inverted values.

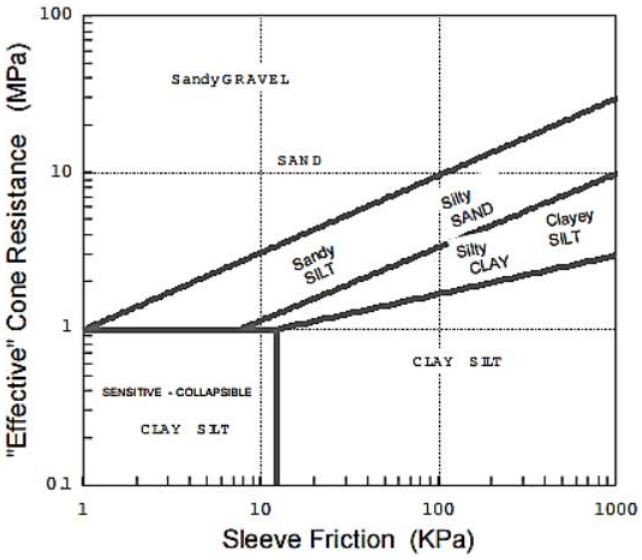

FIGURE 14 ESLAMI AND FELLENIUS PROFILING CHART

2.2 Laboratory tests

2.3.1. Classification analysis

2.3.1.1. Grain-size analysis

The objective of the grain size analysis is to group, in different size classes, the particles constituting the soil and to subsequently determine the weight percentages of each class, referring to the initial weight of the dry material.
The simplest procedure for performing a particle size analysis consists of sieving by means of a series of sieves of gradually decreasing apertures, which must be overlaid and vibrated, in order to separate the granules into fractions of different sizes, each retained at the corresponding sieve.
This method, however, is used exclusively to define the grain size of coarse materials (gravels and sands).
The distribution of granules smaller than 0.075 mm (i.e., the silty particles and clayey) is instead done by indirect methods, which are based on the sedimentation times of the particles in water. In this way it is possible to identify elements as small as the order of the microns, which would be impossible using only the sieves, which typically have a minimum aperture of 0.0075 mm.
In both cases, the result of the test is the grain size curve, a graph where the ordinate is the percent passing to a determine sieve, while the abscissa is the particle diameter.

Dealing with the particle size gradation of fine-grained soils, i.e., the material that pass through the No.200 sieve (opening = 75μm) and larger than about 0.2 μm, the sedimentation (hydrometer) analysis is used.
The concept on which the sedimentation analysis is based on is that the larger particles will fall through a fluid faster than smaller particles. To evaluate the terminal velocity of a spherical particle falling through a stationary liquid the Stokes' Law is used, which is based on several assumptions: the particles are spherical al smooth; there is no interference between the particles; there is no difference between the current in the middle of the containers and the sides; flow is laminar; the particles have the same density.

An important thing to consider is that this test method cannot be applied to some types of soils, such as soils containing fibrous peat, or soils that contain less than 5% of fine-grained material, soils containing extraneous matter (organic solvents, oil, asphalt, wood fragments, or similar items), or materials that contains cementitious components (e.g., cement, fly ash, lime).

As reported in the standard ASTM D7928-17, the first thing to do, in order to perform this test, is the test specimen preparation. Two different methods exist: the moist method and the air-dried one. Moist and air-dried refers to the conditions of the material as it is being reduced to an appropriate particle size and mass. The moist preparation method shall be used for referee testing and for samples not received in the air-dried state, while the air-dried preparation method shall only be used on material received in the air-dried state: this because the air-drying causes irreversible changes to the clay particles that cause permanent flocculation and decreasing in the fine fraction.
The material should be chopped and reduced into small pieces, less than approximately 13mm and mixed to make uniform; in the moist preparation method, test water can be added in order to assist in making uniform sample. If the reduced sample contains particles which are large than 2mm (No.10 sieve), the material must be separated using the No.10 sieve or finer sieve, in order to obtain a representative passing sample. At this point, the amount of moist mass needed for the sedimentation test is evaluated with the following formulation:

$$M_{mest} = H_C * \left(\frac{100}{\%est}\right) * \left(1 + \left(\frac{w_{cest}}{100}\right)\right) \qquad [18]$$

where:

M_{mest} = estimated moist mass

H_C = hydrometer capacity (45g for 151H, 55g for 152H)

$\%est$ = estimated percentage of material passing to the No.200(75μm) sieve

w_{cest} = estimated water content

In the following the procedure that must be follow for the performance of the test is reported:

1. add 5±1 g of sodium hexametaphosphate to the sedimentation specimen in the specimen-mixing container. Sodium hexametaphosphate is a deflocculant agent required to prevent the fine particles in suspension from coalescing or flocculating. Add at least 100mL of test water to the specimen and dispersant to form a slurry of milkshake consistency.

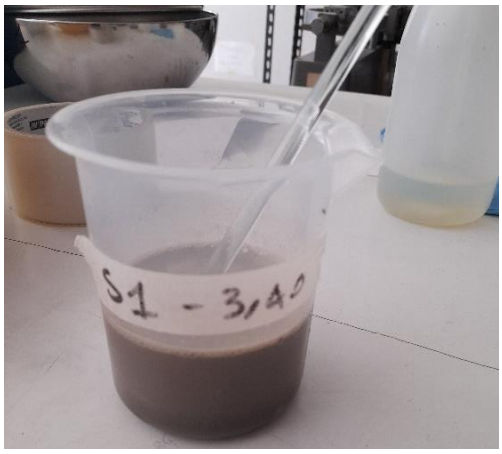

FIGURE 15 SEDIMENTATION SPECIMEN AFTER THE ADDING OF SODIUM HEXAMETAPHOSPHATE

2. Prior to the overnight conditioning period disperse the slurry using the stirring apparatus.
3. Transfer all the dispersed slurry into the sedimentation cylinder, adding test water to bring the bottom of the meniscus of the slurry to the 1000mL±1mm mark.

FIGURE 16 SLURRY INSIDE THE SEDIMENTATION CYLINDER

4. Mixing the slurry using the agitator or the tipping method; the use of tipping method requires a one minute or more tipping, in which the cylinder is turned upside down and back in order to complete the slurry agitation.
5. After a conditioning period of one night mix again the suspension in order to obtain a uniform suspension and put the cylinder immediately in the water bath.

FIGURE 17 SEDIMENTATION CYLINDER INSIDE THE WATER BATH

6. If significant foam develops on top of the suspension after mixing , add up to three drops of isopropyl alcohol (a foam inhibitor)
7. Start the readings at elapsed times, gently placing the hydrometer in the sedimentation cylinder 15-20 seconds before the reading. Record the hydrometer reading r_m and the elapsed time t_m.
8. After the last hydrometer reading is obtained, transfer all the soil suspension to the oven drying container and dry the suspension.
9. Determine and record the dry mass of the soil plus dispersant M_{dd}
10. After the determination of M_{dd} cover the specimen with tap water and allow the specimen to soak.
11. Transfer the soil suspension from the container to the wash sieve
12. Dry the retained material and record the dry mass of the soil retained on the No.200 (75μm) sieve to obtain M_{dr} . during the washing process, the dispersant has been removed, and the resulting dry mass will only include the particles retained on the sieve.

At this point, some calculations must be done in order to determine the percent passing the No.200 (75μm) sieve.

First the dry mass should be evaluated. Two different method exists. The first method is based on the moist mass and water content:

$$M_d = \frac{M_m}{1 + \frac{w_c}{100}} \qquad [19]$$

where:

M_d = mass of dry soil

M_m = mass of moist soil

w_c = water content

The second way to evaluate the dry mass takes into account the oven-dried material as shown in the following equation:

$$M_d = M_{dd} - M_{disp} \qquad [20]$$

where:

M_d = mass of dry soil

M_{dd} = mass of dry soil plus dispersant

M_{disp} = mass of dispersant

Then, the corrected hydrometer reading must be evaluated. Two different equations exist, depending on the type of hydrometer has been used during the test (151H or 152H). Since during this work only the 151H hydrometer has been used, only the equation referring to this hydrometer type is reported.

$$r_{d,m} = A - 7.784 * 10^{-6} * T_m - 4.959 * 10^{-6} * T_m^2 \qquad [21]$$

where:

$r_{d,m}$ = 151H specific gravity hydrometer offset reading *m*

A = average specific gravity shift

T_m = temperature at reading *m*

At this point, for each hydrometer reading taken in the soil suspension, compute the mass of material still in suspension as percentage of the sedimentation specimen, using the right equation depending on the type of hydrometer used. As before, only the equation for the 151H hydrometer is here reported.

$$N_m = \left(\frac{G_s}{G_s - 1}\right)\left(\frac{V_{sp}}{M_d}\right)\rho_c\left(r_m - r_{d,m}\right) * 100 \qquad [22]$$

where:

N_m = mass percent of finer material at reading *m*

V_{sp} = volume of suspension

ρ_c = mass density of water at the temperature of manufacturer calibrated

M_d = dry soil mass of the sedimentation specimen

G_s = specific gravity of the soil

r_m= hydrometer reading in suspension at reading *m*

$r_{d,m}$ = hydrometer offset reading from reference solution at the same temperature as reading *m*

After this, the effective depth is evaluated. This parameter is used in the calculation of the particle fall distance for each hydrometer reading. The following equation is used to calculate the travel distance of the particle when the hydrometer is inserted immediately before a reading and is removed until the next reading:

$$H_m = H_{r2} + \left(\frac{(H_{r1} - H_{r2})}{(r_2 - r_1)} * (r_2 - r_m + C_m)\right) - \left(\frac{V_{hb}}{2A_c}\right) \qquad [23]$$

where:

H_m = distance particles fall at reading *m* when the hydrometer is inserted only for an individual reading

V_{hb} = volume of the hydrometer bulb up to the base of the steam

A_c = cross-sectional area of the sedimentation cylinder

H_r = distance between the centre of (volume) buoyancy and the minimum (H_{r2}) and maximum (H_{r1}) hydrometer readings

r_m = hydrometer reading in suspension at reading *m*

C_m = meniscus correction

r = the minimum (r_2) and maximum (r_1) hydrometer reading

the next to last calculation that must be done is the maximum particle diameter in suspension, that must be evaluated for each hydrometer reading with the following equation:

$$D_m = \left(\sqrt{\frac{18\mu}{\rho_w g(G_s - 1)} * \frac{H_m}{t_m}}\right) * 10 \qquad [24]$$

where:

D_m = particle diameter

μ = water viscosity at 20°C

ρ_w = mass density of water at 20°C

t_m = elapsed (fall) time

H_m= particle fall distance

At the end, the percent passing the No.200(75µm) sieve can be evaluated:

$$P_p = 100\left(1 - \frac{M_{dr}}{M_d}\right) \qquad [25]$$

where:

P_p = percent passing the No.200(75µm) sieve

M_{dr} = initial dry mass of sedimentation specimen without dispersant

M_d = dry mass retained on the No.200(75µm) sieve

2.3.1.2. Atterberg limits

Another important classification analysis is the determination of Atterberg limits.

This type of tests is made because the particle size gradation gives only quantitative information, and it is not possible to obtain information about the characteristics of clay minerals, which for example in the case of cohesive materials, are of prevailing importance because they affect their physical-mechanical behaviour. The latter, in the case of clays, is closely related to the presence of water, which is absorbed by the individual particles creating more or less strong bonds.

When a certain amount of water is added to a dried clayey soil, a thin film of adsorbed water is created around the particles: the increase of the amount of water produces the increase of the water thickness, which at a certain point allows the particles to flow each other.

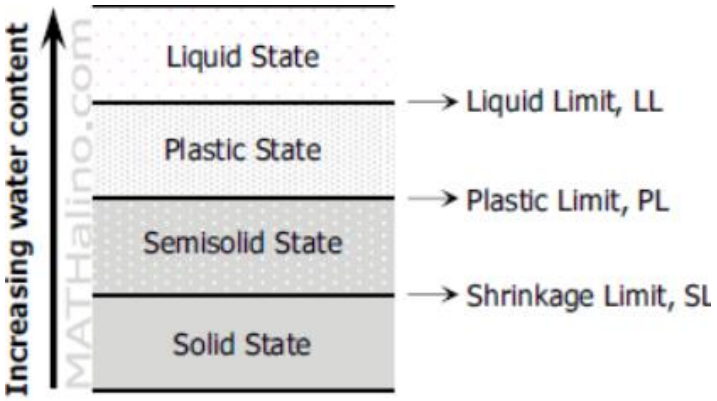

FIGURE 18 ATTERBERG LIMITS REPRESENTATION

The fine-grained soils can be found in 4 different consistency states, depending on the water content. Atterberg limits define the moisture contents at which fine-grained clay and silt soils transition between solid, semi-solid, plastic, and liquid states occur.
The Atterberg limits are three:

- Liquid Limit (LL): is the water content at which soil changes from a plastic to a liquid state when the soil specimen is just fluid enough for a groove to close when jarred in a specified manner.
- Plastic Limit (PL): is the water content at the change from a plastic to a semi-solid state. This test involves repeatedly rolling a soil sample into a thread until it reaches a point where it crumbles.
- Shrinkage Limit (SL): is the water content where the further loss of moisture does not cause a decrease in specimen volume.

The determination of the liquid limit and plastic limit are done following the ASTM D4318; below the procedure to be observed for the evaluation of these parameters is reported.

- Liquid Limit (LL)

Thoroughly remix the specimen (soil) in its mixing cup, and, if necessary, adjust its water content until the constancy requires about 25 to 35 blows of the liquid limit device to close the groove. Using a spatula, place a portion of the prepared soil in the cup of the liquid limit device at the point where the cup rests on the base, squeeze it down, and spread it into the cup to a depth of about 10 mm at its deepest point, tapering to form an approximately horizontal surface. Take care to eliminate air bubbles from the soil pat but form the pat with as few strokes as possible. Form a groove in the soil pat by drawing the tool, bevelled edge forward, through the soil on a line joining the highest point to the lowest point on the rim of the cup. When cutting the groove, hold the grooving tool against the surface of the cup and draw in an arc, maintaining the tool perpendicular to the surface of the cup throughout its movement.

FIGURE 19 GROOVED SOIL PAT ON LL DEVICE

At this point, start to lift and drop the cup by turning the crank at a rate of 1.9 to 2.1 drops per second until the two halves of the soil pat come in contact at the bottom of the groove along a distance of 13 mm (1⁄2 in.) and record the number of drops, *N*, required to close the groove.
Remove the soil and repeat the test with the same soil specimen but with an increased water content by adding distilled water: the increase of the water content should determine a decrease of the number of blows required to close the groove. This procedure should be repeated for at least other two times, producing successively lower numbers of blows to close the groove. One of the trials shall be for a closure requiring 25 to 35 blows, one for closure between 20 and 30 blows, and one trial for a closure requiring 15 to 25 blows.
Now, determine the water content, W_n , of the soil specimen from each trial, drying in oven at a temperature of 110°C±5°C the specimen. The water content is given by the ratio between the wet specimen and the dried specimen multiplied by 100.
The evaluation of the liquid limit is obtained plotting the relationship between the water content, W_n, and the corresponding number of drops, *N*, on a semilogarithmic graph with the water content as ordinates on the arithmetical scale, and the number of drops as abscissas on a logarithmic scale. Draw the straight line through the three or more plotted points. Take the water content corresponding to the intersection of the line with the 25-drop abscissa as the liquid limit of the soil.

- Plastic Limit (PL)

The plastic limit is determined taking 20 g or more portion of soil from the material prepared for the liquid limit test. The water content of the soil must be reduced until a consistency at

which it can be rolled without sticking to the hands is reached. The drying process may be accelerated by exposing the soil to the air. Start to roll the mass between the palm or fingers and the ground-glass plate with just sufficient pressure to roll the mass into a thread of uniform diameter throughout its length. The thread shall be further deformed on each stroke so that its diameter reaches 3.2 mm (1⁄8 in.), taking no more than 2 min. Typically fragile soils of low plasticity are best rolled under the outer edge of the palm or at the base of the thumb.

At this point the specimen is weighted and the water content is evaluated as before. This procedure must be repeated for 2 times. The plastic limit is evaluated as the average between the water content of the two specimens.

Once the Liquid and Plastic Limits have been determined, the plasticity index can be evaluated:

$$PI = LL - PL \qquad [26]$$

2.3.1.3. USCS classification

The Unified Soil Classification System (USCS), defined by the standard regulation ASTM D2487, is a method used to classify mineral and organo-mineral soils for engineering purposes, based on laboratory determination of particle-size characteristics, liquid limit, and plasticity index.

This classification system identifies three major soil divisions: coarse-grained soils, fine-grained soils, and highly organic soils. These three divisions are further subdivided into 15 basic soil groups.

To determine the USCS class of fine-grained soils and fine-grained fractions of coarse-grained soils, a Plasticity Chart is required. A typical plasticity chart is shown in Figure 20.

Major division			Group symbol	Typical name	Classification criteria	
Coarse-grained soils (More than 50% retained on No. 200 ASTM sieve)	Gravels 50% or more of coarse fraction retained on No. 4 ASTM sieve	Clean gravels	GW	Well-graded gravels and gravel-sand mixtures, little or no fines.		$U = D_{60}/D_{10}$ greater than 4 $C_c = D^2_{30}/(D_{60} \times D_{20})$ between 1 and 3.
			GP	Poorly-graded gravels and gravel-sand mixtures, little or no fines.	Classification on the basis of percentage of fines. Less than 5% passing No. 200 ASTM sieve—GW, GP, SW, SP. More than 12% passing No. 200 ASTM sieve— GM, GC, SM, SC. 5% to 12% passing No. 200 ASTM sieve—Border-line classification requiring use of dual symbols.	Not meeting both criteria for GW.
		Gravels with fines	GM	Silty gravels, gravel-sand-silt mixtures.		Atterberg limits plot below *A*-line or plasticity index less than 4.
			GC	Clayey gravels, gravel-sand-clay mixtures.		Atterberg limits plot above *A*-line or plasticity index less than 4.
	Sands More than 50% of coarse fraction passes No. 4 ASTM sieve	Clean sands	SW	Well-graded sands and gravelly sands, little or no fines.		U greater than 6 C_c between 1 and 3.
			SP	Poorly-graded sands and gravelly sands, little or no fines.		Not meeting both criteria for SW.
		Sands with fines	SM	Silty sands, and-silt mixtures.		Atterberg limits plot below *A*-line or plasticity index less than 4.
			SC	Clayey sands, sand-clay mixtures.		Atterberg limits plot above *A*-line or plasticity index greater than 7.
Fine-grained soils (50% or more passes No. 200 ASTM Sieve)	Silts and Clays (Liquid limit 50% or less)		ML	Inorganic silts, very fine sands, rock flour, silty or clayey fine sands.	Check Plasticity Chart	
			CL	Inorganic clays or low to medium plasticity, gravelly clays, sandy clays, silty clays, lean clays.		
			OL	Organic silts and organic silty clays of low plasticity.		
	Silts and clays (Liquid limit greater than 50%)		MH	Inorganic silts, micaceous or diatomaceous fine sands or silts, elastic silts.		
			CH	Inorganic clays of high plasticity, fat clays.		
			OH	Organic clays of medium to high plasticity.		
Highly organic clays			P_t	Peat, muck and other highly organic soils.	Fibrous organic matter, will char, burn, or glow. Readily identified by colour, odour, spongy feel, and fibrous texture.	

Note: Boundary classification: Soils possessing characteristics of two groups are designated by combinations of group symbols — for example, GW-GC, well-graded, gravel-sand mixture with clay binder

FIGURE 20 USCS CLASSIFICATION CHART

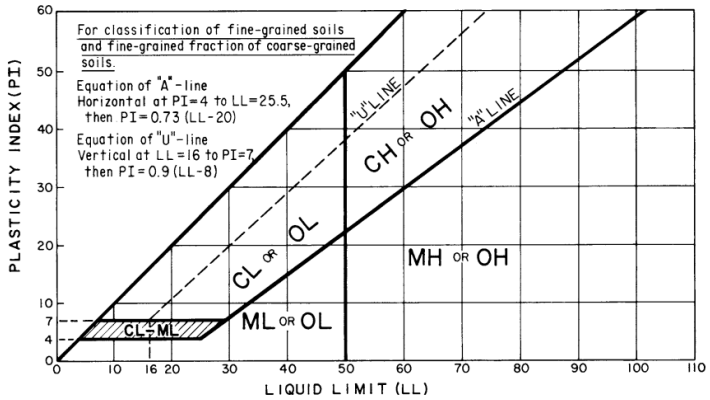

FIGURE 21 PLASTICITY CHART

Based on results of visual observations and laboratory tests, a soil can be defined according to a basic soil group, assigning a group symbol(s) and name, and thereby classified.

The following schemes report the flow charts to classify a soil, starting from its grain-size characteristics, in particular depending on its passing to the No. 200 sieve (75μm).

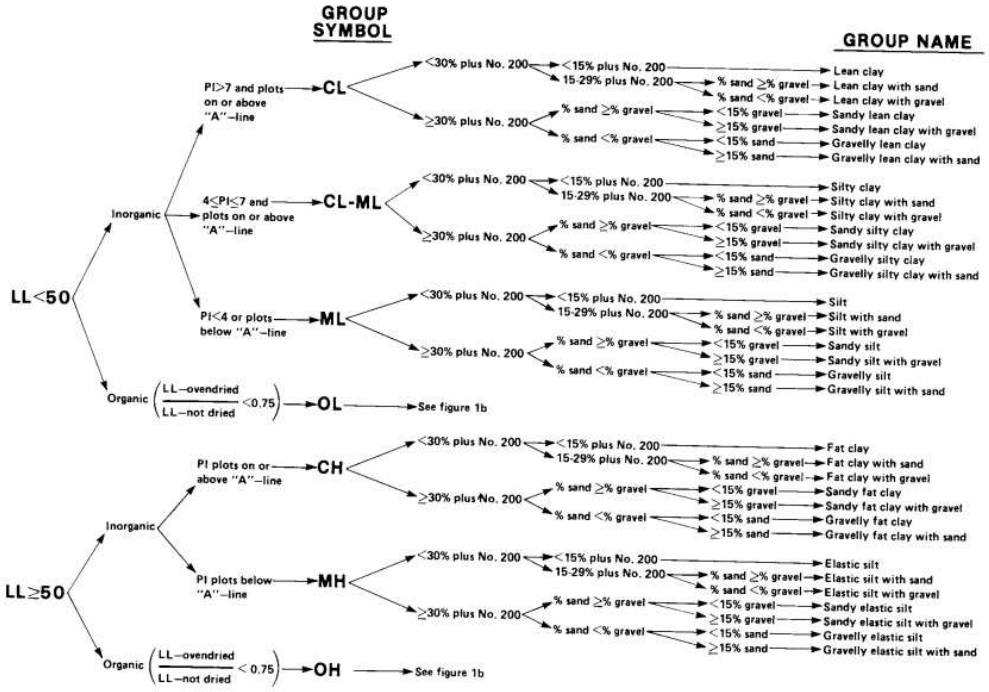

FIGURE 22 FLOW CHART FOR FINE-GRAINED SOILS (50% OR MORE PASSING TO THE NO.200 SIEVE)

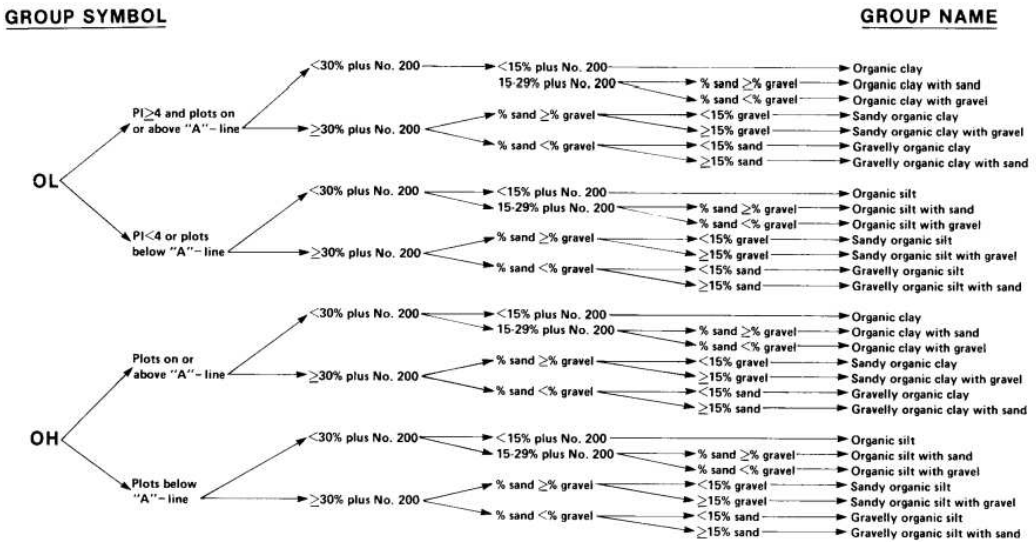

FIGURE 23 FLOW CHART FOR ORGANIC FINE-GRAINED SOILS (50% OR MORE PASSING TO NO.200 SIEVE)

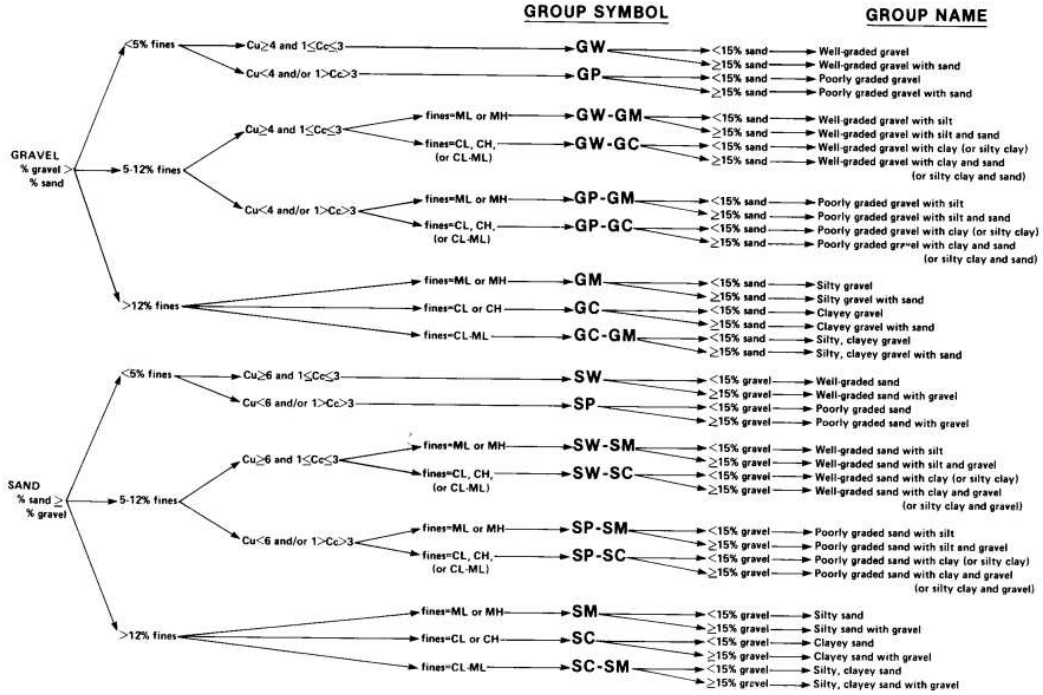

FIGURE 24 FLOW CHART FOR COARSE-GRAIN SOILS (50% OR MORE RETAINED TO NO.200 SIEVE)

2.4. Triaxial test

The triaxial test is one of the most versatile of all the methods for testing the shear strength of a soil. It can measure the total and effective stress parameters, and it can be performed on any type of soil. Drainage can be controlled, and pore water pressure and volume changes can be measured accurately. Three main types of triaxial tests exist:

- Unconsolidated undrained test (UU)
- Consolidated undrained test (CU)
- Consolidated drained test (CD)

In general, a consolidated triaxial test is divided into 2 phases: during the first phase an isotropic or anisotropic stress is applied, and this phase can be identified as Consolidated (C); during the second phase, the specimen is brought to a breaking point, applying vertical stress, and this phase can be in Drained conditions (D) or Undrained conditions (U).

For the UU test, the specimens (assumed to be saturated prior to test) are subjected to a confining fluid pressure in a triaxial chamber. Once the specimen is inside the triaxial cell, the cell pressure is increased to a predetermined value and the specimen is brought to failure by increasing the vertical stress by applying a constant rate of axial strain. Since saturation and consolidation do not exist in this method, original structure and water content of sample remain constant. Pore and back pressures are not measured during this test and therefore the results can only be interpreted in terms of total stress.

These tests are generally carried out on three specimens of the same sample subjected to different confining stresses. Since all specimens are supposedly saturated the shear strength are similar for all tests.

The results of the test are plotted as curves of principal stress difference against strain. For conditions of maximum principal stress difference (taken as failure) Mohr circles are plotted in terms of total stress. The average undrained shear strength is recorded, and the failure (Mohr) envelope is drawn tangential to the Mohr circles in order to find the “undrained cohesion intercept” and undrained “angle of shearing resistance”.

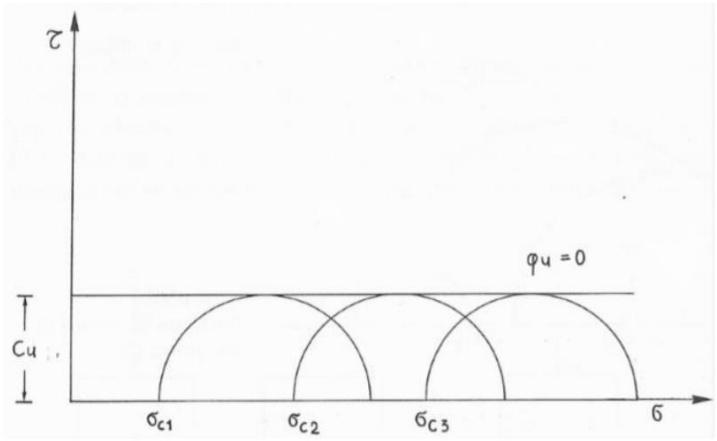

FIGURE 25 FAILURE ENVELOP (UU)

For the CD and CU tests, peak effective strength parameters (c' and φ') can be determined either from the results of consolidated undrained (CU) triaxial compression tests with pore pressure measurement or from consolidated drained (CD) triaxial compression tests. The consolidated undrained/drained triaxial compression tests are normally performed in several stages, involving the successive saturation, consolidation and shearing of each of three specimens.

Saturation is carried out in order to ensure that the pore fluid in the specimen does not contain free air. Saturation is normally carried out by leaving the specimens to an elevated back pressure so that the air in the pores is dissolved in water. Back pressure (which is an imposed pore pressure) is applied through a volume change gauge to the top of the specimen, while a cell pressure of slightly higher value is also applied. Both cell pressure and back pressure are normally increased in increments, allowing time for equalization at each stage. The degree of saturation can be expressed in terms of Skempton's pore pressure parameter (Skempton, 1954):

$$B = \frac{\Delta u}{\Delta \sigma 3} \qquad [27]$$

where Δu is equal to change in pore pressure for an applied cell pressure change of Δσ3. For an ideally saturated soil, B is equal to 1.

The consolidation phase of an effective stress triaxial test is carried out for two reasons: first, three specimens are tested and consolidated at three different effective pressures, in order to give specimens of different strengths which will produce widely spaced effective stress Mohr circles; secondly, the results of consolidation are used to determine the minimum time to failure in the shear stage.

For the CIU test, once consolidation is complete, the specimen must be isolated from the back pressure and the rate of vertical movement of the compression machine platen set according to

result of consolidation. During the shear stage the vertical stress is increased by the loading ram and measurements are made at regular intervals of deformation, ram load and pore pressure. These are converted to graphs of principal stress difference (σ1- σ3) and pore pressure as a function of strain, and failure is normally taken as the point of maximum principal stress difference. The effective stress Mohr circles are plotted for the failure conditions of the three specimens which has been subjected to different consolidation level, and the gradient and intercept of a straight line drawn tangential to these circles defines the effective strength parameters *c′* and *φ*'.

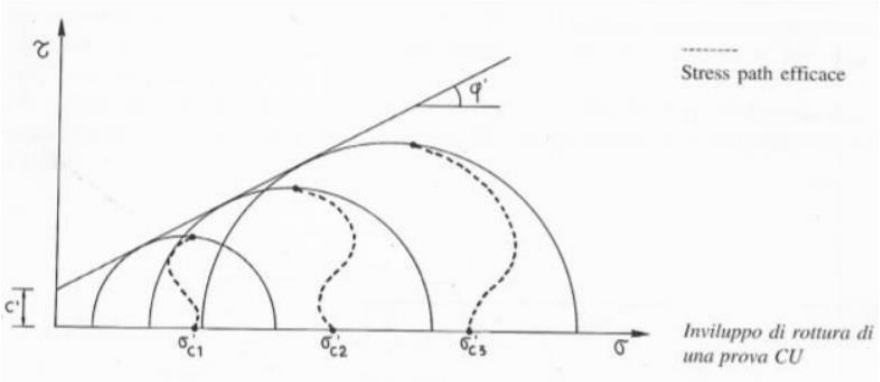

FIGURE 26 FAILURE ENVELOP (CIU)

While for CD test, volume change measurement during shear is carried out in a similar sequence to the consolidated undrained test, but during shear the back pressure remains connected to the specimen which is loaded sufficiently slowly to avoid the development of excess pore pressures. The shear stage of a drained triaxial test can be expected to take between 7 and 15 times longer than that of an undrained test with pore pressure measurement.

Once shearing is complete, the results are presented as graphs of principal stress difference and volume change as a function of strain, and the failure Mohr circles are plotted to give the drained failure envelope defined by the parameters *cd′* and *φd′* .

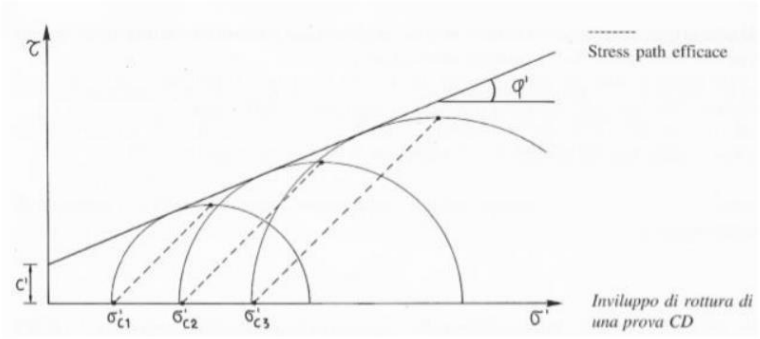

FIGURE 27 FAILURE ENVELOPE (CD)

2.3. Oedometer test

These test methods cover procedures for determining the magnitude and rate of consolidation of soil when it is restrained laterally and drained axially while subjected to incrementally applied controlled-stress loading.

A soil specimen is restrained laterally and loaded axially with total stress increments. Each stress increment is maintained until excess pore water pressures are essentially dissipated. Pore pressure is assumed to be dissipated based on interpretation of the time deformation under constant total stress. This interpretation is founded on the assumption that the soil is 100% saturated. Measurements are made of change in the specimen height and these data are used to determine the relationship between the effective axial stress and void ratio or strain. When time deformation readings are taken throughout an increment, the rate of consolidation is evaluated with the coefficient of consolidation.

The procedure for the test execution can be found in the ASTM D2435/D2435M, and it is reported in the following.

Assemble the ring with specimen, porous disks, filter screens (when needed) in the consolidometer. If the specimen will not be inundated shortly after application of the seating load, enclose the consolidometer in a loose-fitting plastic or rubber membrane to prevent change in specimen volume due to evaporation.

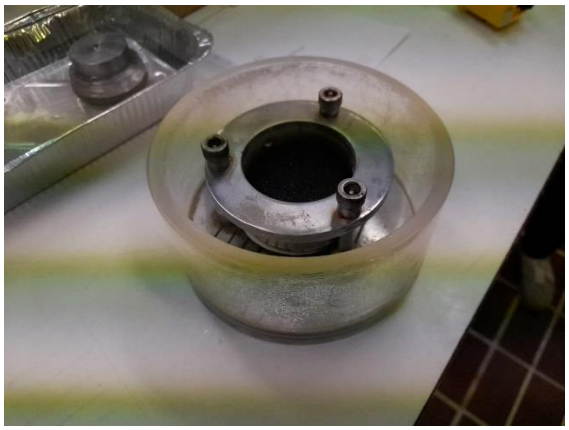

FIGURE 28 PREPARATION OF THE SPECIMEN

1. Place the consolidometer in the loading device and apply a seating load that results in a total axial stress of about 5 kPa. Immediately after application of the seating load, adjust the deformation indicator and record the initial deformation reading, do.

2. If the test is performed on an intact specimen that was either saturated under field conditions or obtained below the water table, inundate with the test water shortly after application of the seating load. As inundation and specimen wetting occur, quickly increase the load as required to prevent swelling.

3. The specimen is to be subjected to load increments of constant total axial stress. The standard loading schedule shall consist of a load increment ratio (LIR) of one which is obtained by approximately doubling the total axial stress on the soil to obtain values of about 12, 25, 50, 100, 200, etc. kPa

4. Before each load increment is applied, record the height, or change in height, d_f, of the specimen. For each increment, record the axial deformation, *d*, at time intervals of approximately 0.1, 0.25, 0.5, 1, 2, 4, 8, 15, 30 min, and 1, 2, 4, 8 and 24 h. The standard load increment duration shall exceed the time required for completion of primary consolidation.

5. To minimize swell during disassembly, rebound the specimen back to the seating load (corresponding to a total axial stress of about 5 kPa). Once the change in axial deformation has reduced to less than 0.2 % per hour (usually overnight), record the end-of-test axial deformation, det and remove the consolidometer from the load frame quickly after releasing the final small seating load on the specimen. Remove the

specimen and the ring from the consolidometer and wipe any free water from the ring and specimen.

6. Measure the height of the specimen Het, to the nearest 0.01 mm by taking the average of at least four evenly spaced measurements over the top and bottom surfaces of the specimen using a dial comparator.

7. Determine the final total mass of the specimen, M_{Tf} to the nearest 0.01 g, by measuring the soil plus the ring and subtracting the tare mass of the ring.

8. Determine the specimen dry mass M_d and water content w_f, using the entire specimen.

2.4. Diffractometry

Diffractometry is a qualitative analysis in which X-rays are used to determine the crystal structure of materials. It is an experimental method in which a beam of X-ray is made to pass through a sample of the material being tested. Since the atoms are arranged in some order in crystals, they tend to diffract the beam at certain angles and at certain intensity.

In particular, as it is reported in the standard regulation ASTM D934-22, a powdered sample is irradiated with a monochromatic X-ray beam of short wavelength (from about 0.05 to 0.25 nm). The X rays interact with the atoms in the crystal and are scattered in a unique diffraction pattern which produces a fingerprint of the crystal's atomic or molecular structure.

The holder containing the specimen is rotated through an angle of θ deg while the detector receiving the diffracted beam is rotated through 2θ deg. A random number of crystallites in the powdered specimen will be so oriented that they will obey the Bragg equation ($n\lambda = 2d \sin \theta$). The intensity and the angle of the diffracted beam can be either recorded on a strip chart or digital printer. The data from the sample under investigation may be evaluated by comparison with published data and identification can be made. The recorded intensity pattern of a certain deposit may provide some quantitative data, but often, only experience with known types of deposits or using internal standards can produce accurate quantitative results.

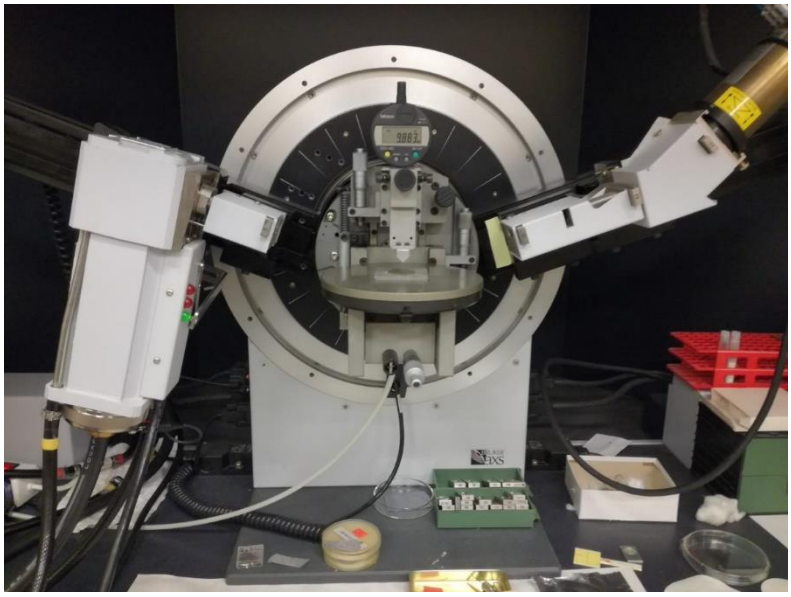

FIGURE 29 X-RAY DIFFRACTOMETER

IV. UNDRAINED SHEAR STRENGTH FROM CPT

The interpretation of the undrained shear strength (C_u) of fine-grained soils from CPT and CPTU results has been widely studied, and a large amount of works have been proposed in the literature. In general, two main approaches of interpretation exist, one based on theoretical solutions, and the other based on empirical correlations.

Theoretical solutions can be grouped in five different classes:

- Classical bearing capacity theory
- Cavity expansion theory
- Conservation of energy combined with cavity expansion theory
- Analytical and numerical approaches using linear and non-linear stress-strain relationship
- Strain path theory.

Regardless of the theory considered, all theoretical solutions are based on the relationship between the cone resistance q_c and the undrained shear strength C_u in the following form:

$$q_c = N_c * C_u + \sigma_o \qquad [28]$$

where:

N_c is the theoretical cone factor

σ_o is the in-situ total pressure.

The main limitation of the theoretical solutions is that they apply several simplifying assumptions to soil behaviour, failure mechanism and boundary conditions, and these solutions must be verified from field and/or laboratory tests. For this reason, empirical correlations are generally preferred, although the theoretical solutions have provided a useful framework of understanding (Lunne et al. 1997).

Empirical approaches available for the interpretation of C_u from CPT or CPTU results can be divided into 3 main categories:

- Cu estimation using total cone resistance
- Cu estimation using effective cone resistance
- Cu estimation using excess pore pressure.

In the following these 3 methodologies will be analysed.

4.1. C_u estimation using total cone resistance

The estimation of C_u from CPT using cone resistance is made using the following equation:

$$C_u = \frac{q_c - \sigma_{vo}}{N_k} \qquad [29]$$

where N_k is an empirical cone factor and σ_{vo} is the total in situ vertical stress.
Over the years several studies have been done for the evaluation of the N_k value.
Kjekstad *et al*. (1978) showed that for non-fissured overconsolidated clays, with C_u from triaxial compression tests as the reference strength, an average value of N_k was 17. Lunne and Kleven (1981) showed that for normally consolidated marine clays with field vane as reference test, the cone factor N_k varied from 11 to 19 with an average value of 15.

An improvement of this approach, using CPTU results, is to employ the corrected cone resistance q_t; in this way, the cone factor is expressed as follow:

$$N_{kt} = \frac{q_t - \sigma_{vo}}{c_u} \qquad [30]$$

Even in this case, many studies have been performed, and the main results are reported.
Aas et al. (1986) defined N_{kt} value considering the average value of Cu :

$$C_{u,lab} = \frac{c_{uc} + c_{ud} + c_{ue}}{3} \qquad [31]$$

where c_{uc} is the undrained shear strength from triaxial compression, c_{ud} is the undrained shear strength from direct simple shear, and c_{ue} is the undrained shear strength from triaxial extension test. Moreover, they found that N_{kt} increases when the plasticity increases (Fig. 30), and the values of N_{kt} varies between 8 and 16 when the plasticity index (I_p) varies between 3 and 50%.

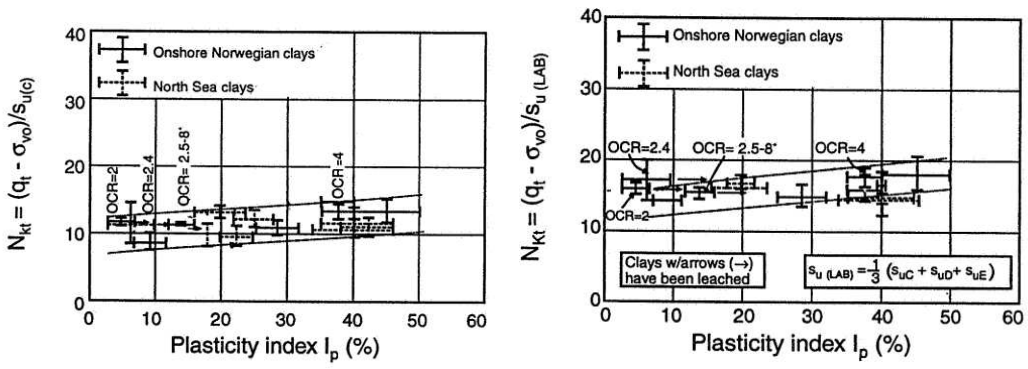

FIGURE 30 COMPUTED CONE FACTOR NKT VS IP

Conversely, La Rochelle et al. (1988) did not find a correlation between N_{kt} and I_p, and they showed that N_{kt} varied between 11 and 18.

Rad and Lunne (1988) demonstrated that using C_u from triaxial compression tests as reference strength, the N_{kt} values vary from 8 to 29, with the OCR being the main variable.

Powell and Quarterman (1988) showed that N_{kt} based on triaxial compression shear strength varies from 10 to 20 depending on I_p (in a similar way to the Aas results). They also showed that when scale effects were considered, especially in fissured clays, the range of N_{kt} increased to 10-30.

Over the years many studies have been performed, and the in general two main aspects must be considered:

- It is crucial to specify which method is used to determine the C_u value, because the measured C_u value varies depending on many factors, among which the testing method.
- The effect of sample disturbance: the less disturbed the sample, the higher is the undrained shear strength and the lower is the N_{kt} factor.

4.2. C_u estimation using effective cone resistance

Senneset et al. (1982) proposed the use of the effective cone resistance q_e for the interpretation of C_u, where q_e is given by the difference between the measured cone resistance and the pore pressure measured behind the cone (u_2). Campanella et al. (1983) redefined the effective cone resistance by using the corrected cone resistance q_t, obtaining the following equation:

$$C_u = \frac{q_t - u_2}{N_{ke}} \qquad [32]$$

This correlation was obtained for normally to lightly overconsolidated clays and it should not be extrapolated to heavy overconsolidated deposits (Powell and Quarterman, 1988). In general, this correlation works well, but it is not recommended for soft normally consolidated clays, since in such soils the total pore pressure generated behind the cone is often approximately 90% or more of the measured cone resistance. A major disadvantage of using q_e to evaluate C_u in such soils, is that q_e is a very small quantity, sensitive to small errors in q_c or u measurements (Lunne et al., 1997).

4.3. C_u estimation using excess pore pressure

Using theoretical and semi-theoretical approaches based on cavity expansion theory, a number of relationships have been proposed between excess pore pressure Δu and C_u (Vesic 1972; Battaglio et al., 1981). The relationship has the following form:

$$C_u = \frac{\Delta u}{N_{\Delta u}} \qquad (\Delta u = u_2 - u_0) \qquad [33]$$

Based on cavity expansion, $N_{\Delta u}$ is theoretically shown to assume values between 2 and 20. Many studies were performed, and the main results are reported in the following.
Lunne et al. (1985) found $N_{\Delta u}$ to correlate well with B_q and to vary from 4 to 10 for North Sea clays, taking triaxial compression strength as reference strength. La Rochelle et al. (1988), using uncorrected field vane strength as reference strength, found that for three Canadian clays $N_{\Delta u}$ varied from 7 to 9, even if the OCR ranged from 1.2 to 50.

In general, talking about empirical correlations, piezocones should be used wherever possible; it is important to point out that the use of site-specific empirical correlations is the best procedure for the interpretation of C_u from CPT/CPTU tests.
Based on the above discussion, the evaluation of C_u from CPT/CPTU data in cohesive fine-grained soils, should take account of the following aspects:

- For deposits where little experience is available, estimate C_u using the total cone resistance q_t, and preliminary cone factor values (N_{kt}) from 15 to 20. For a more conservative estimate, select the value closer to the upper limit. For normally and lightly overconsolidated clays N_{kt} can be as low as 10 and in stiff fissured clay can be as high as 30. In very soft clays, where there can be some uncertainty with the accuracy of q_t,

estimate C_u with the excess pore pressure (Δu_2) measured behind the cone using $N_{\Delta u}$ from 7 to 10. For a more conservative estimate, select a value closer to the upper limit.

- If previous experience is available in the same deposit, the values suggested above should be adjusted to reflect this experience.
- For larger projects, where high-quality field and laboratory data may be available, site-specific correlations should be developed based on appropriate and reliable values of C_u.

V. RESULTS

Empirical correlations are largely used in geotechnical problems and in the specific case of the Ancona CDF, a site-specific correlation between the undrained shear strength C_u and the penetration resistance q_c is proposed. In the literature, such a correlation has been proposed by using the cone factor that can vary over a large range depending on geology and soil type. In this case, the empirical correlation has been attempted starting from the results obtained with the CPTU tests, applying the method based on N_{kt}.
It is important to stress that this empirical correlation is site specific, and all the calculation can only be referred to the examined sediments.

To obtain the site-specific empirical correlation related to the first sector of the Ancona CDF, the procedure used is the following:

1. Elaboration of CPTU results and identification of the stratigraphic units (only CPTU results were used for the purpose)
2. Identification of the fine-grained stratigraphic units (characterized by soil behaviour type index I_c > 2.6) in order to define boundaries for which the empirical correlation is valuable
3. Use of laboratory tests on samples taken in the adjacent borehole to verify that the stratigraphic units were actually formed by fine-grain soils
4. Triaxial test to obtain the undrained shear strength (C_u)
5. Elaboration of the empirical correlation, using the Eq. 30, for the definition of the site-specific cone factor values.

5.1. CPTU results

As said in Cap.1, after the consolidation phase, 6 piezocone tests were performed. The results are expressed in terms of cone resistance (q_t), friction ratio (f_r) and pore pressure (u) along the depth (up to a depth of 6 m, where the test was stopped). The numerical values have been

worked out on several Excel files, and the results are reported for all the CPTUs performed on the test pad of the CDF's first sector (Figs. 31 to 36).

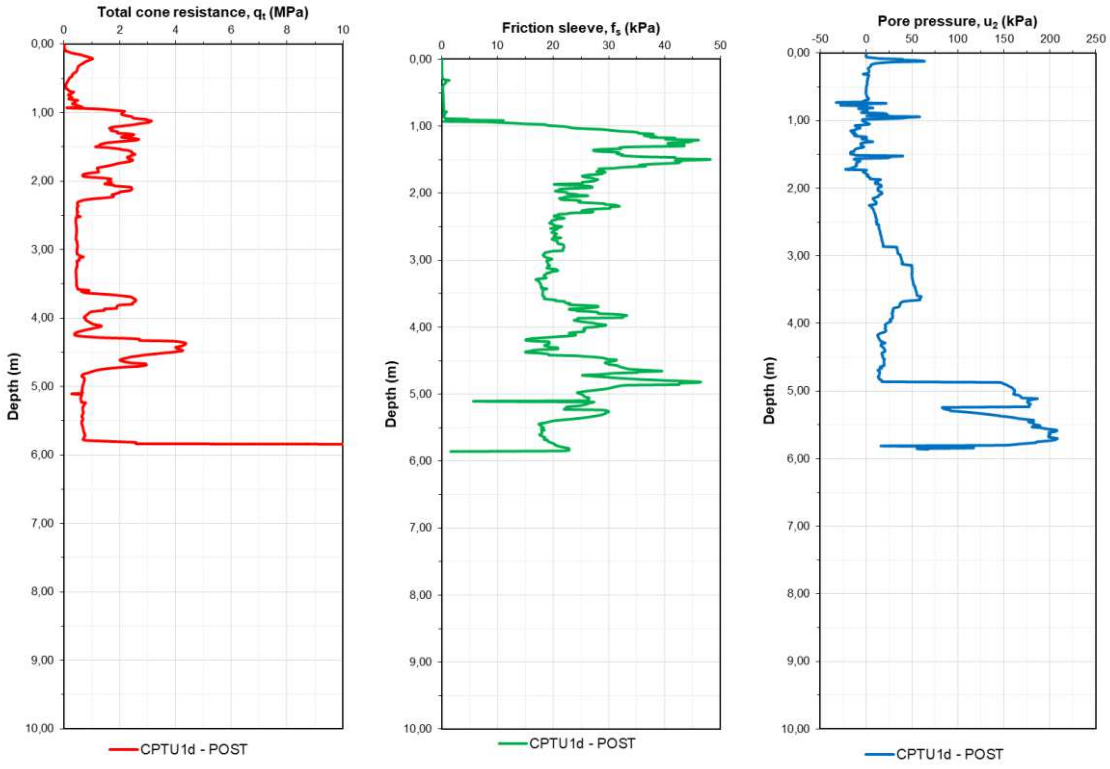

FIGURE 31 CPTU1 POST RESULTS

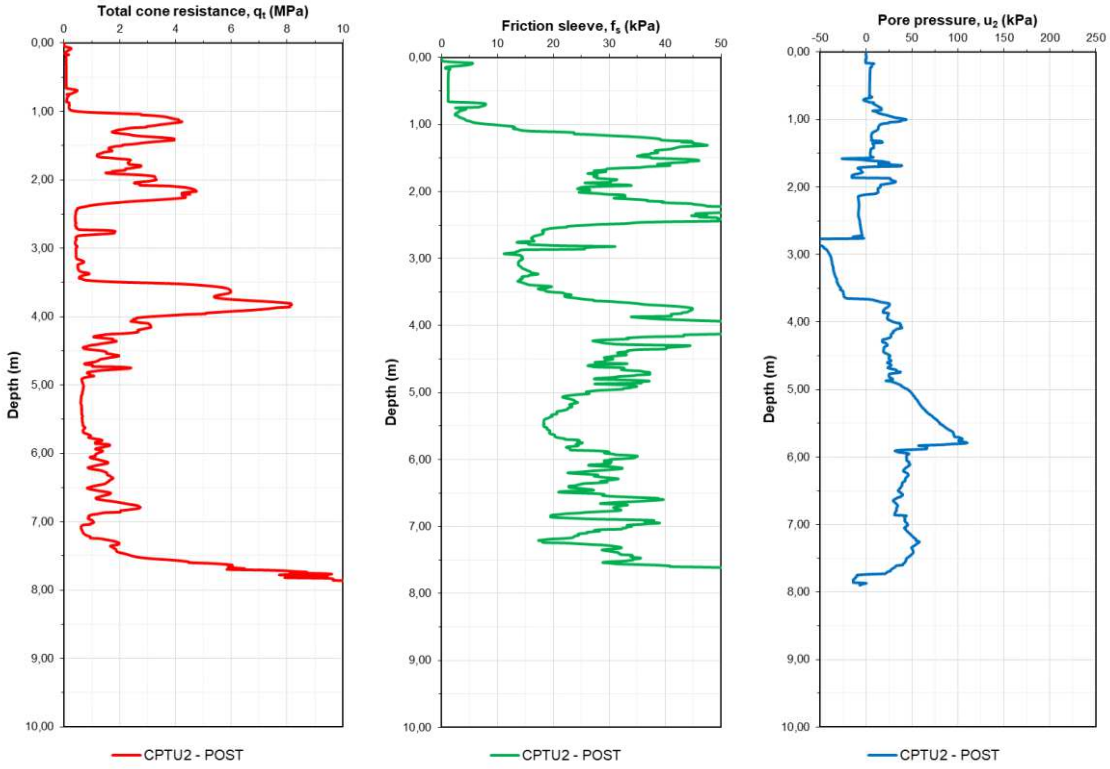

FIGURE 32 CPTU2-POST RESULTS

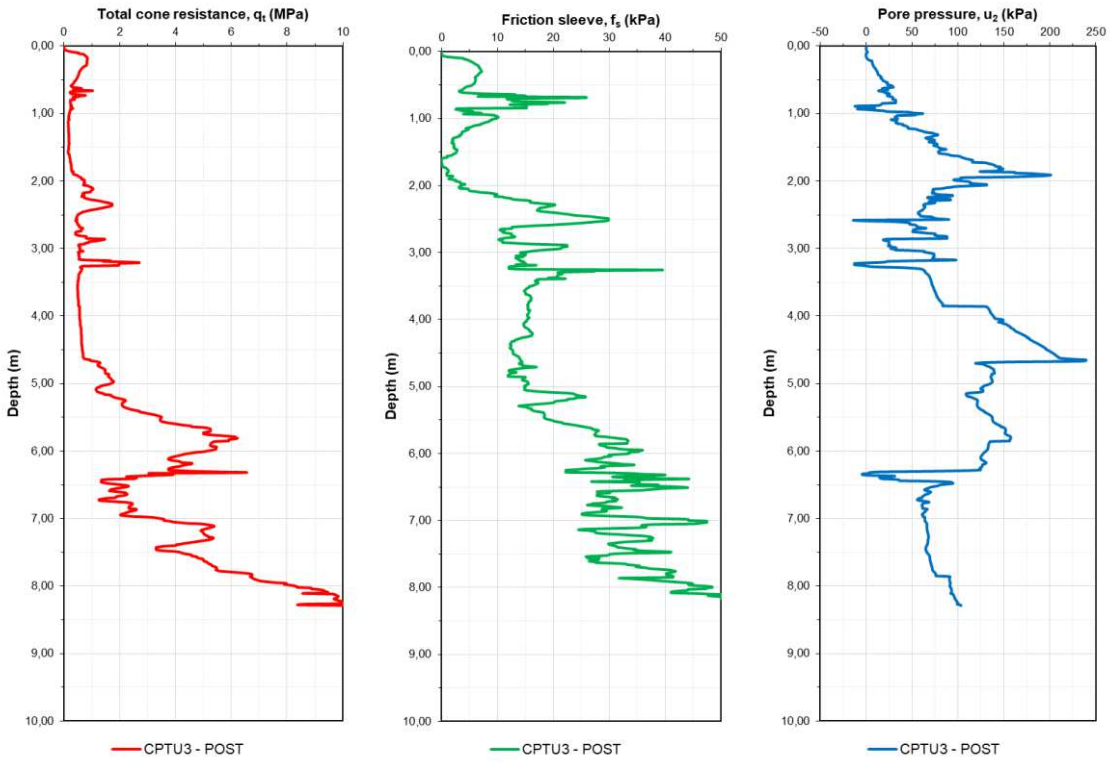

FIGURE 33 CPTU3 POST RESULTS

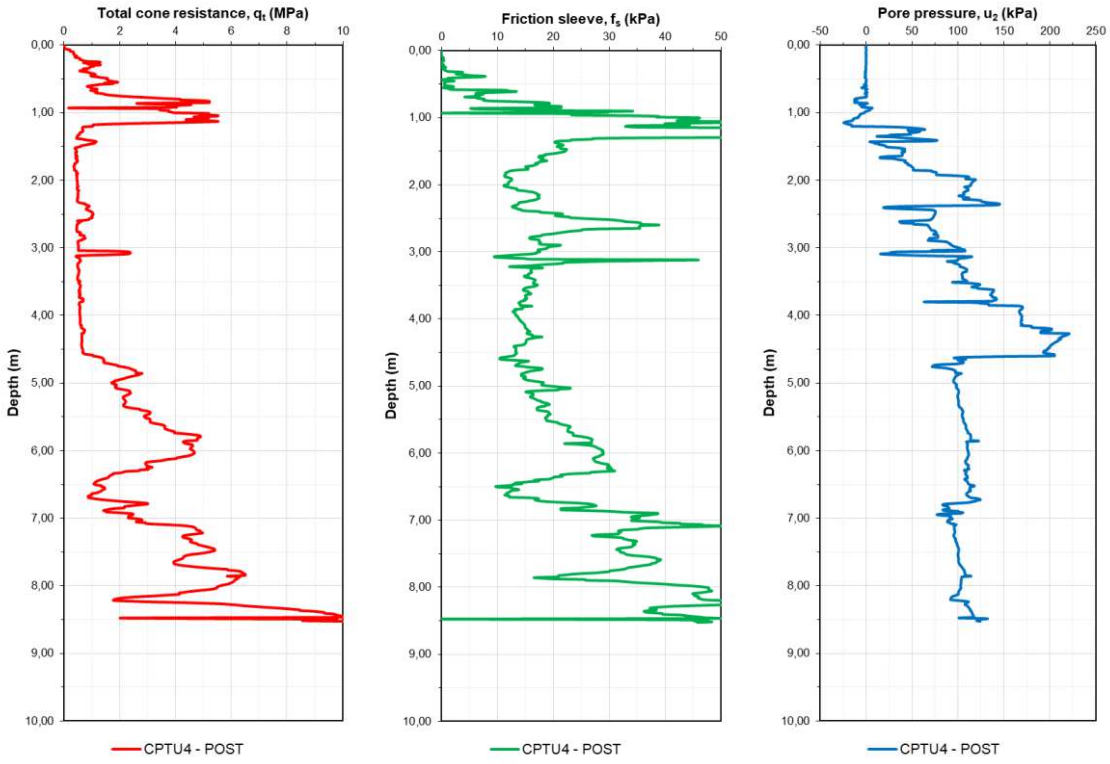

FIGURE 34 CPTU4 POST RESULTS

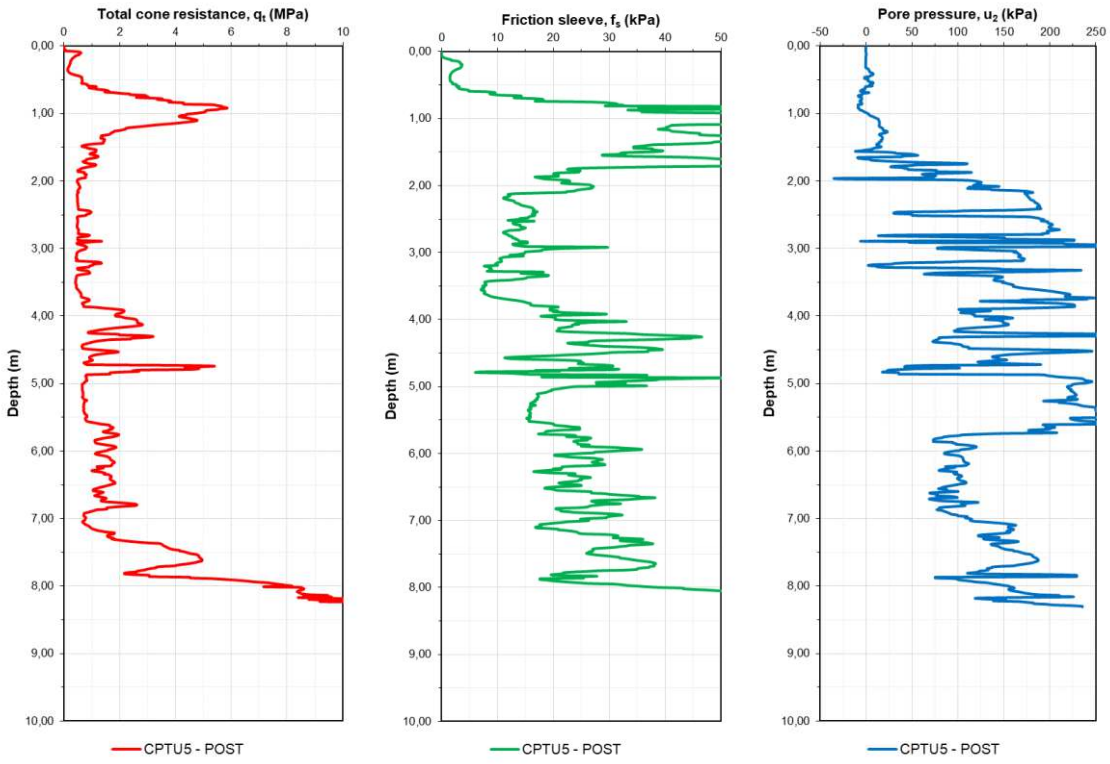

FIGURE 35 CPTU5 POST RESULTS

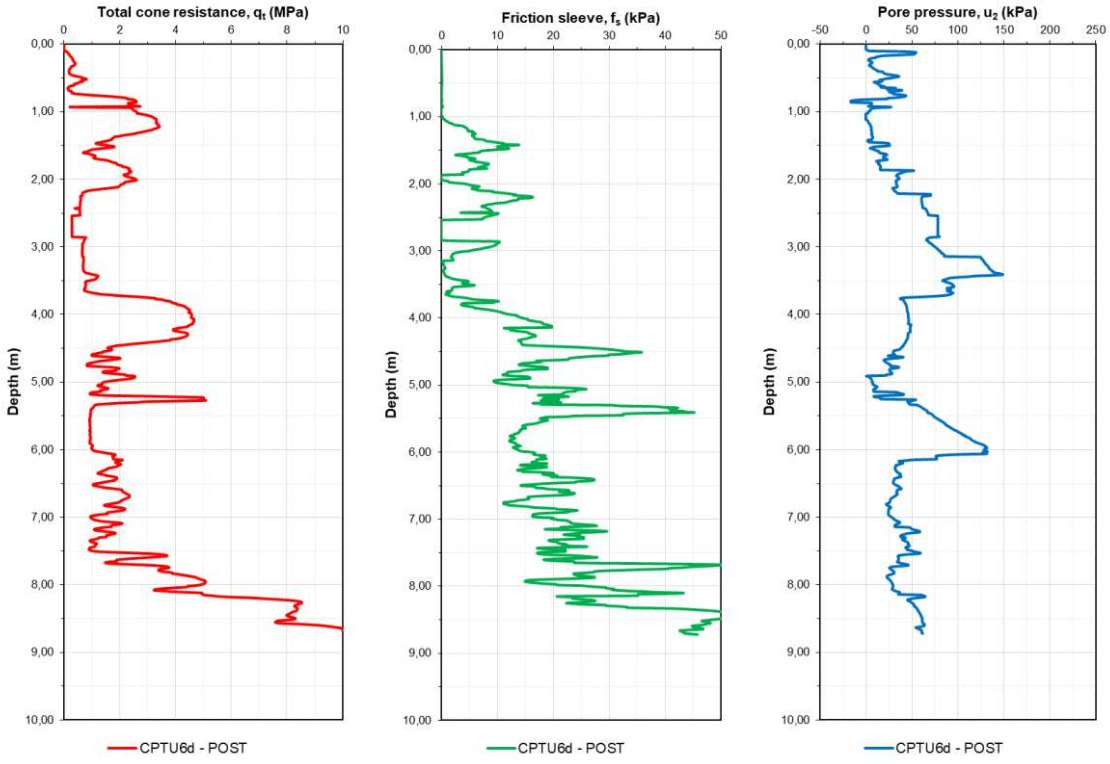

FIGURE 36 CPTU6 POST RESULTS

As can be observed in the first graph of all the CPTUs (q_t graph), a rough qualitative definition of the different stratigraphic units can be made by considering q_t values: the highest values correspond to coarse-grained sediments (mostly sands) in correspondence of which a drop of pore pressure occurs, while lower q_t values correspond to the fine-grained sediments.
This aspect can be further explored with the evaluation of the soil behaviour type index I_c: if the I_c is higher than 2,6 that soil will be classified as a clay-like, and vice versa, if the I_c is lower than 2,6 that soil will be classified as sandy-like.

Considering that only the results from CPTU1 (in the central vertical axis of the embankment footprint) have been analysed (even dealing with laboratory test), from here onward this work will be referred only to these data.
To obtain a clearer and more comprehensible reading of the results, it was decided to subdivide the whole depth into 5 layers with more or less similar values of cone resistance. To each layer a colour was assigned, and these results were reported on the classification charts.
In the following the Robertson SBT chart referred to non-normalized (Robertson SBT chart of 2010) and normalized data (Robertson SBTn charts of 2009 and 2016), and the Eslami and Fellenius chart are reported.

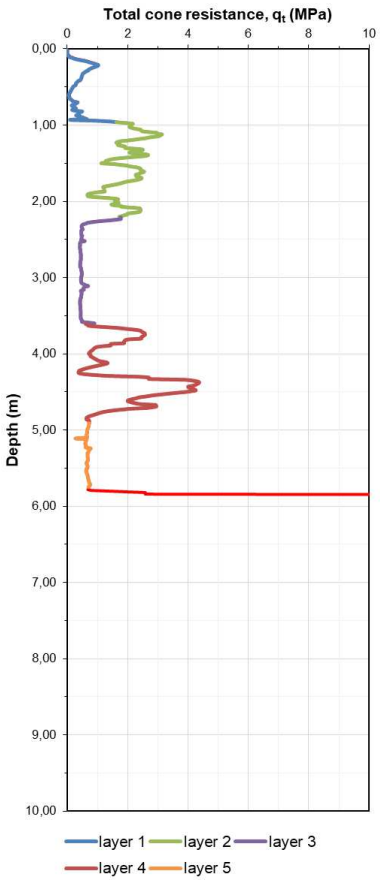

FIGURE 37 LAYERS SUBDIVISION

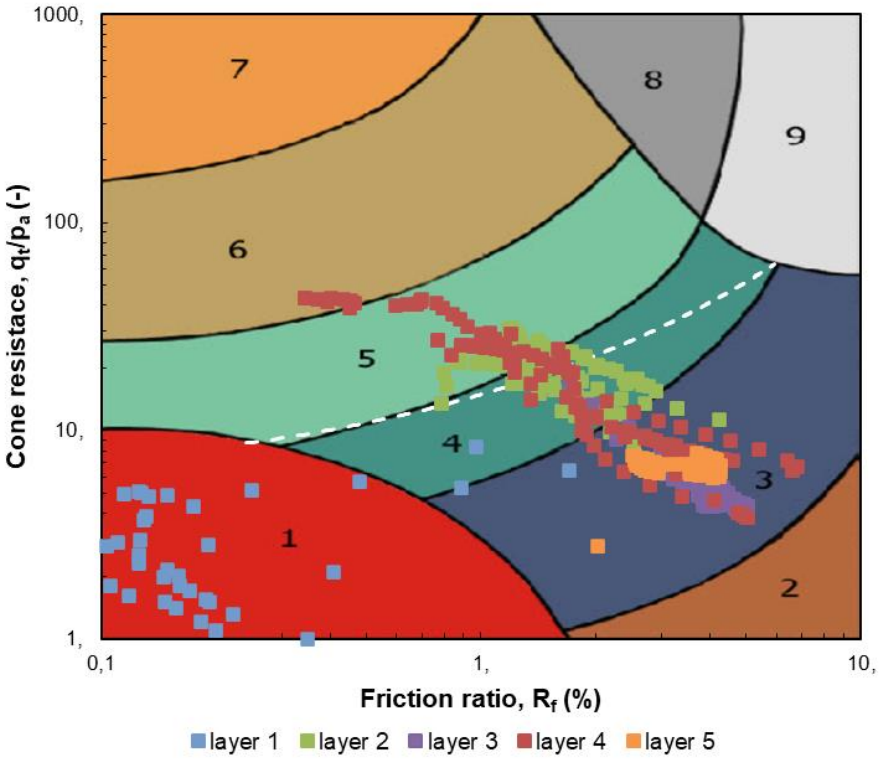

FIGURE 38 SBT CHART (ROBERTSON 2010) FOR CPTU1

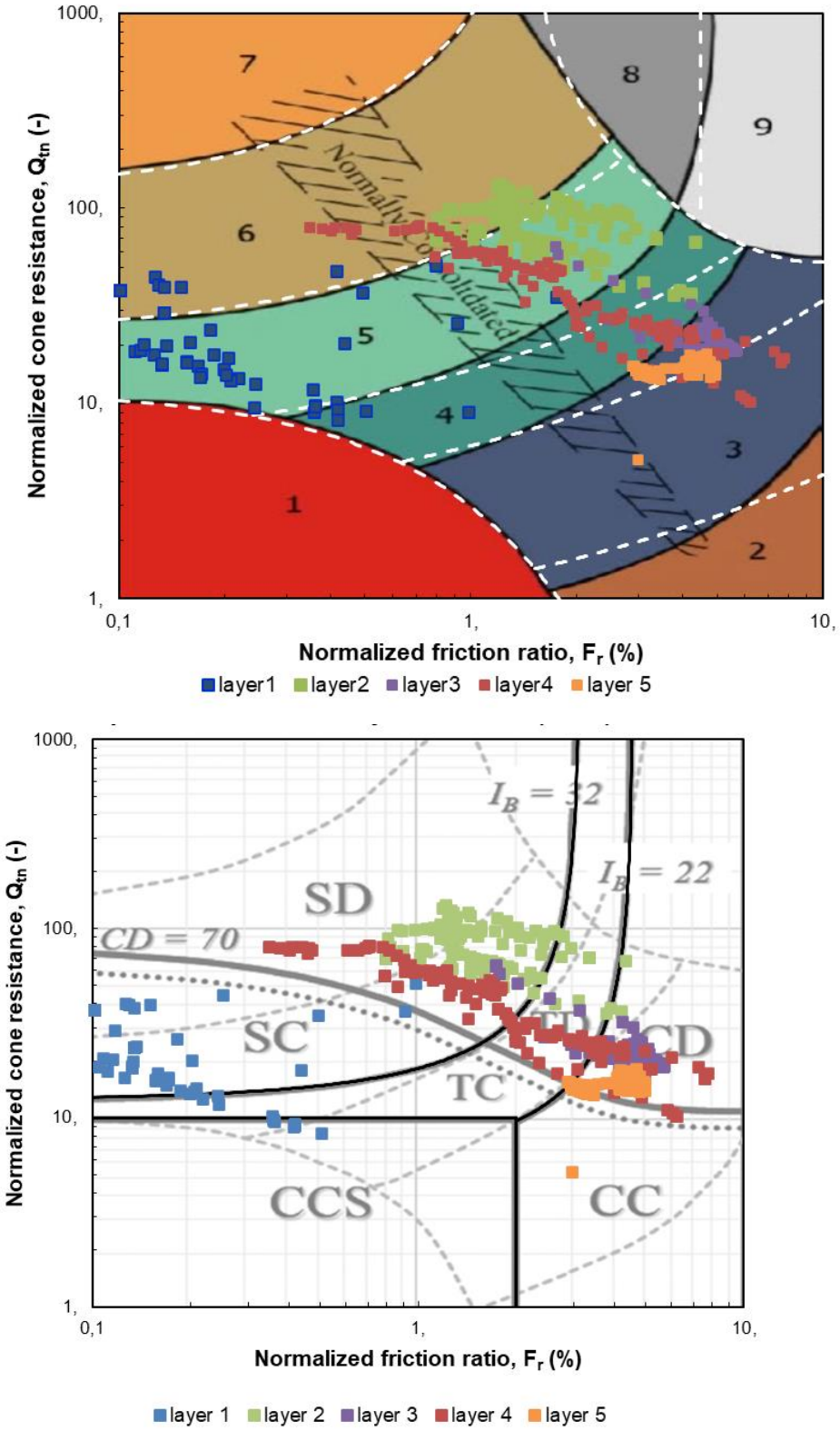

FIGURE 39 SBT CHART: (A)ROBERTSON 2009, (B) ROBERTSON 2016 (NORMALIZED PARAMETERS) FOR CPTU1

As can be observed in the first SBT chart (Robertson 2010), the predominant soil behaviour is the one of clay soils and silt mixtures (being the most part of the points inside zone 3 and 4). From the SBT chart referred to normalized parameters (Robertson 2009), it can be noticed that the main behaviour type is the one referred to silty mixtures (zone 4) and sand mixtures (zone 5).
If the 2016 Robertson SBT chart is considered, this deposit can be characterized as a likely dilative, being all the point above the CD=70 line.

A more intuitive graph, based on normalized parameters, is plotted in Fig. 40: this graph shows identification of fine-grained soils and coarse-grained soils along the depth considering the soil behaviour index I_c . The red line identifies the I_c value equal to 2.6, and the curve reported on the right side of the red line highlights a fine-grained deposit, while the curve reported on the left side of the red line means that the deposit is characterised by coarse-grained material. Each section is identified by a different colour, that represents the belonging soil behaviour type.
In particular, only 2 layers ("layer 3" and "layer 5") are characterized by an I_c value higher than 2.6, and how it will be seen in the following chapters, in these two parts of the vertical (from 2.61 m to 3.60 m and from 4.91 m to 5.75 m) the empirical correlation for the determination of the cone factor will be applied.

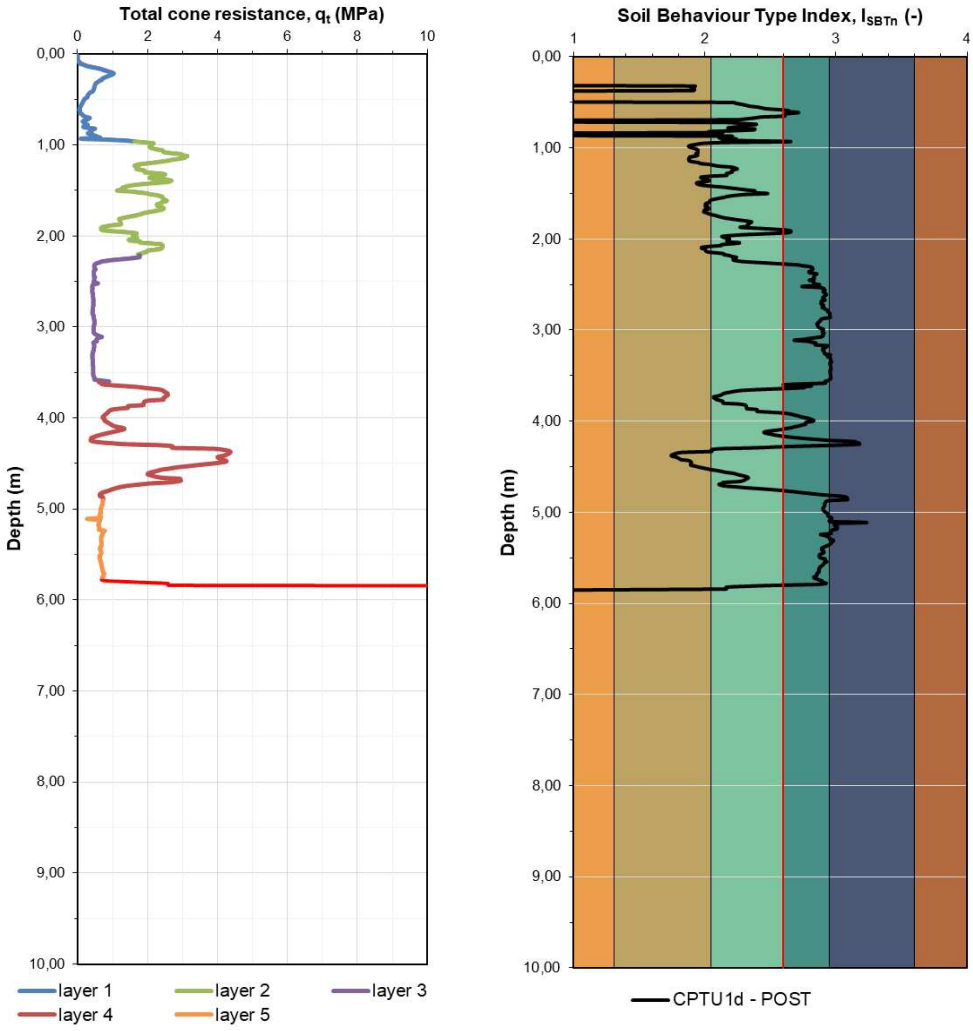

SBTn chart based on normalized data	
SBT Zone	**Soil behaviour type description**
9	Very stiff, fine grained*
8	Very stiff sand to clayey sand*
7	Gravelly sand to sand
6	Sands: clean sand to silty sand
5	Sand mixtures: silty sand to sandy silt
4	Silt mixtures: clayey silt & silty clay
3	Clays: clay to silty clay
2	Organic soils: peat
1	Sensitive, fine-grained

FIGURE 40 SBT ALONG THE DEPTH

Another interpretation of CPTU results is given by Eslami and Fellenius SBT chart. As can be seen in Fig. 41, also this classification chart gives the same results even if other parameters are considered (q_e instead of q_t or Q_{tn}).

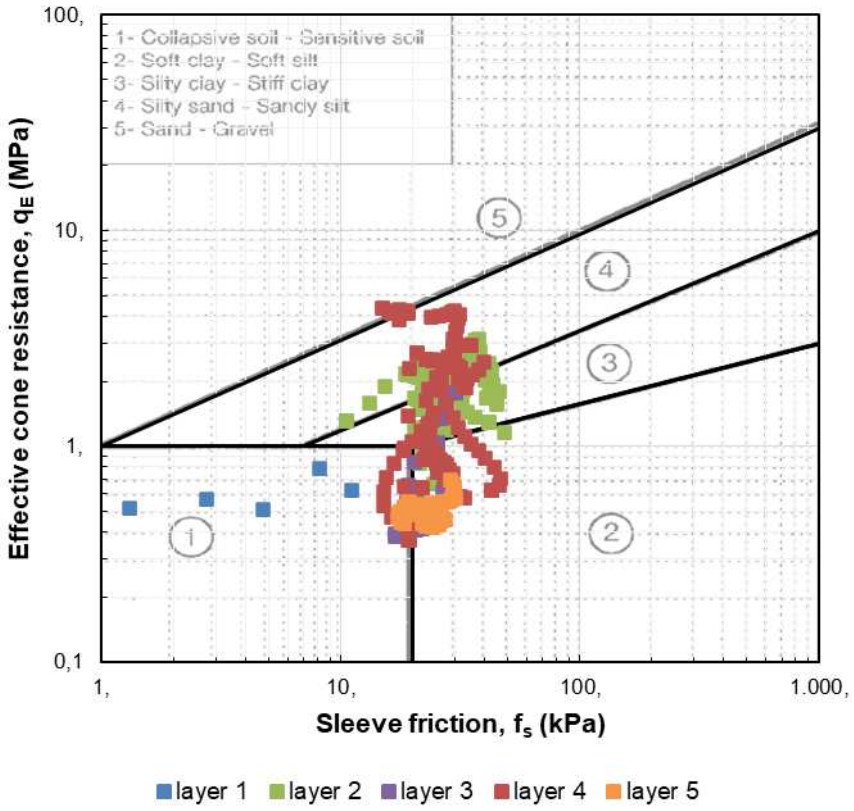

FIGURE 41 ESLAMI AND FELLENIUS SBT CHART FOR CPTU1

In Fig.42, the above SBT charts are reported only for the layer 3 and layer 5.

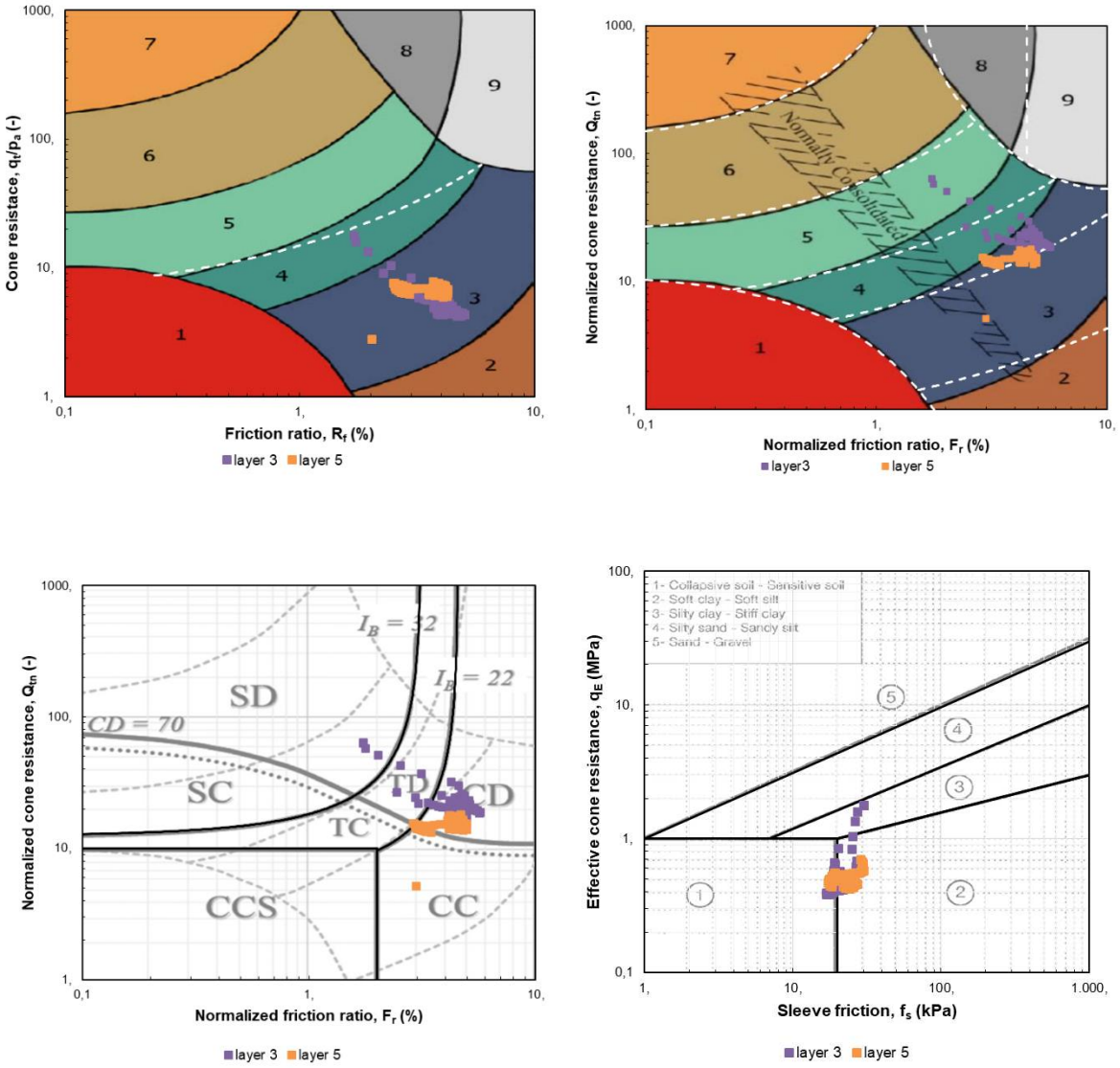

FIGURE 42 SBT CHARTS FOR LAYER 3 AND LAYER 5

These outcomes can be confirmed by the laboratory tests done to identify the grain size of some reference samples taken in the interesting layers as detailed in the following section.

5.2. Classification analysis

The samples considered were taken at different depths and depending on the type of soil available two different methodologies were used: the sedimentation (hydrometer) analysis for

fine-grained portion of the soil and sieve analysis for coarse-grained one. Table 4 reports the samples analysed, the corresponding depth and the test method used (CR means Remoulded Sample and CI undisturbed sample). All the results obtained are reported in the following tables and figures.

TABLE 4 TESTED SAMPLES FOR GRAIN-SIZE ANALYSIS (CR = REMOULDED SAMPLE, CI = UNDISTURBED SAMPLE;)

SAMPLE	DEPTH(m)	GRAIN-SIZE ANALYSIS
S1-CR-1.30	1.3	sedimentation analysis+sieving
S1-CR-2.30	2.3	sedimentation analysis
S1-CR-3.40	3.4	sedimentation analysis
S1-CR-3.90	3.9	sedimentation analysis
S1-CI-4.50	4.5	sedimentation analysis
S1-CR-5.30	5.3	sedimentation analysis
S1-CI-6	6	sieving

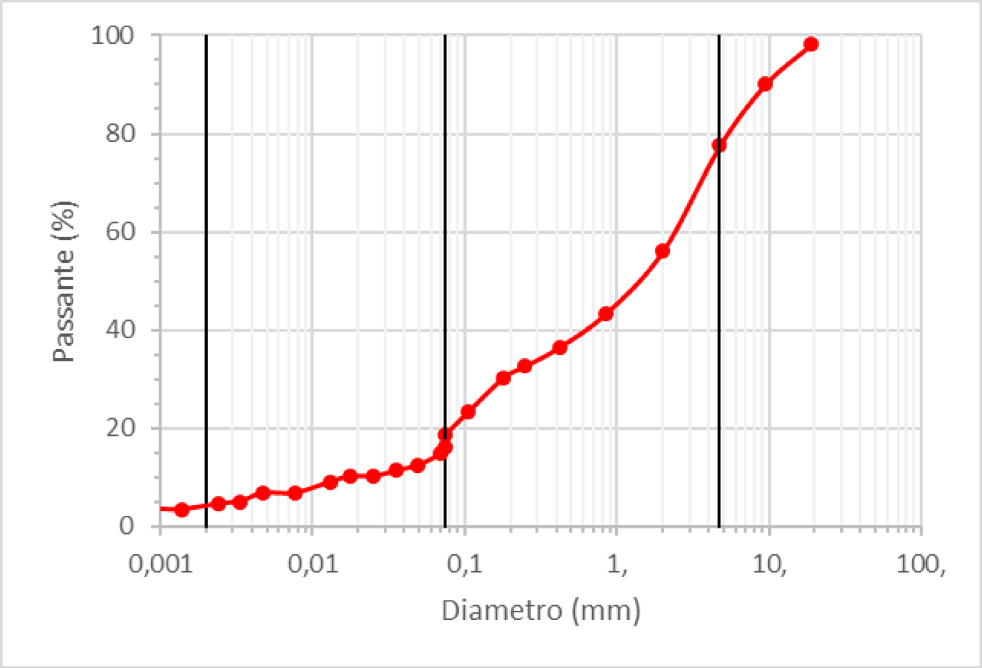

FIGURE 43 GRAIN-SIZE CURVES FROM SEDIMENTATION ANALYSIS AND DRY SIEVING (S1-CR-1.30)

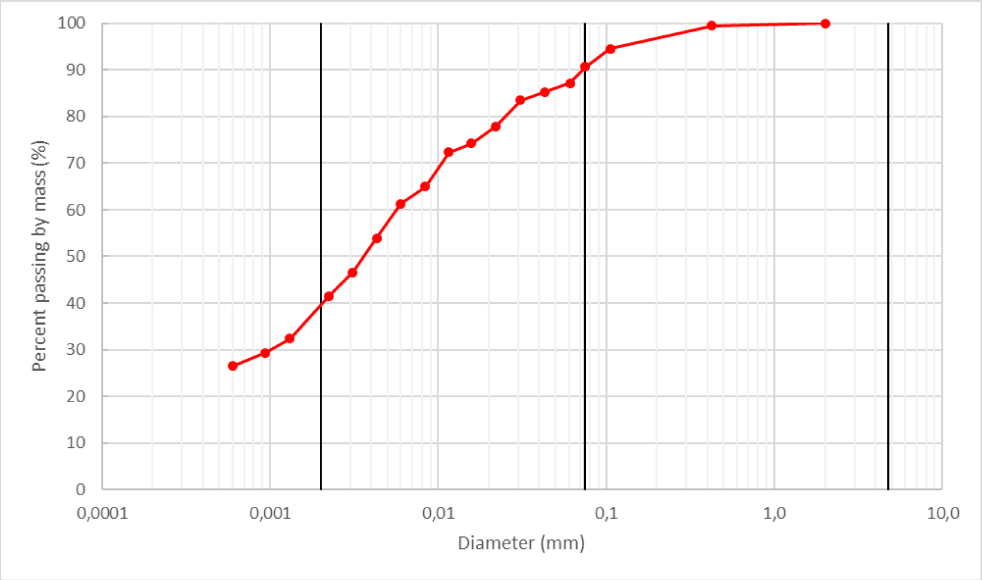

FIGURE 44 GRAIN-SIZE CURVE FROM SEDIMENTATION ANALYSIS AND WET SIEVING (S1-CR-2.30)

TABLE 5 S1-CR-2.30 FRACTIONS FROM SEDIMENTATION ANALYSIS

Coarse	%	9.3
gravel	G %	0.0
sand	S %	9.3
Fine	%	90.7
silt	M %	51.1
clay	CF %	39.6

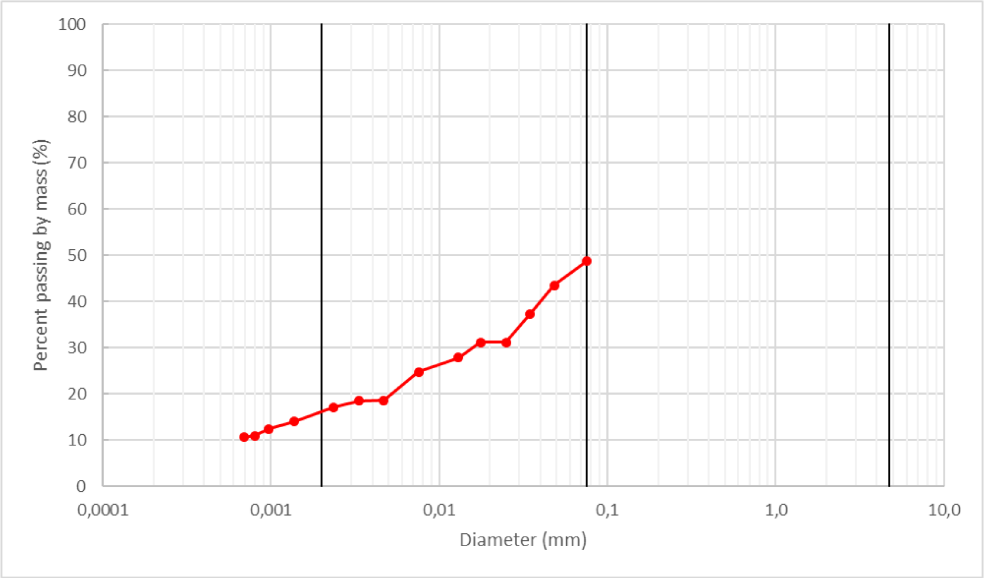

FIGURE 45 GRAIN-SIZE CURVE FROM SEDIMENTATION ANALYSIS AND WET SIEVING (S1-CR-3.40)

TABLE 6 S1-CR-3.40 FRACTIONS FROM SEDIMENTATION ANALYSIS

Coarse	%	51.4
gravel	G %	0.0
sand	S %	51.4
Fine	%	48.6
silt	M %	32.5
clay	CF %	16.1

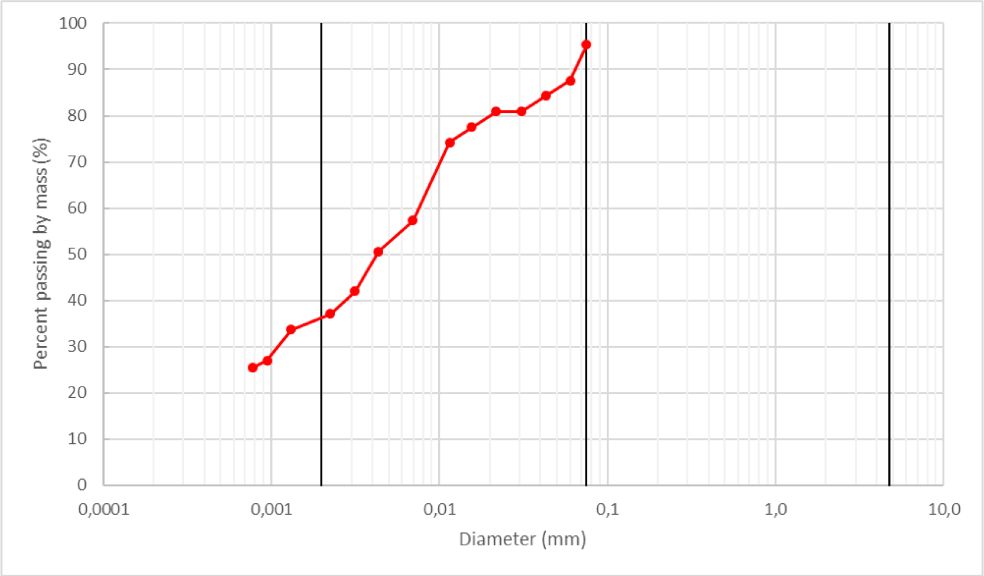

FIGURE 46 GRAIN-SIZE CURVE FROM SEDIMENTATION ANALYSIS AND WET SIEVING (S1-CR-3.90)

TABLE 7 S1-CR-3.90 FRACTIONS FROM SEDIMENTATION ANALYSIS

Coarse	%	4.6
gravel	G %	0.0
sand	S %	4.6
Fine	%	95.4
silt	M %	59,0
clay	CF %	36.4

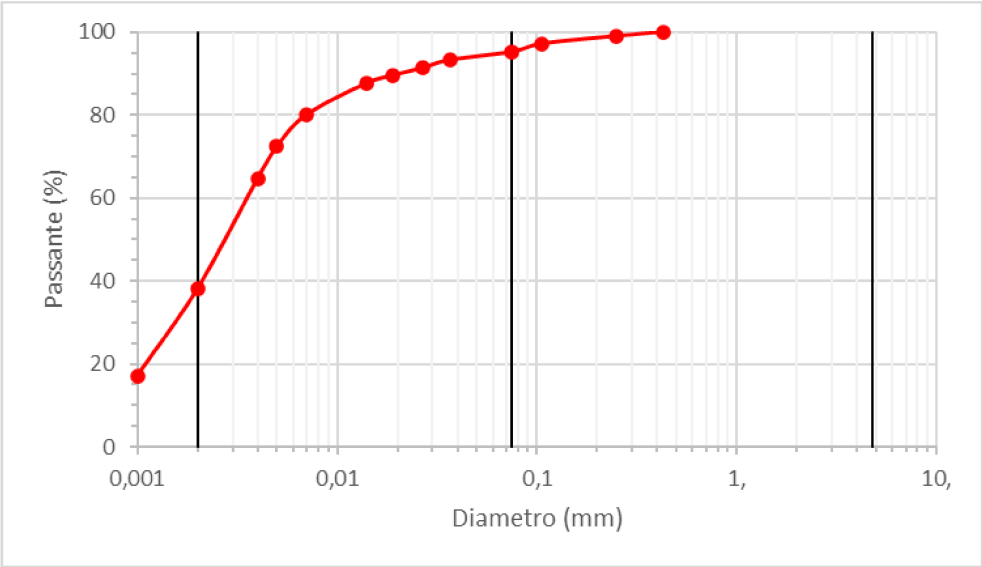

FIGURE 47 GRAIN SIZE CURVE FROM DRY SIEVING (4,5M)

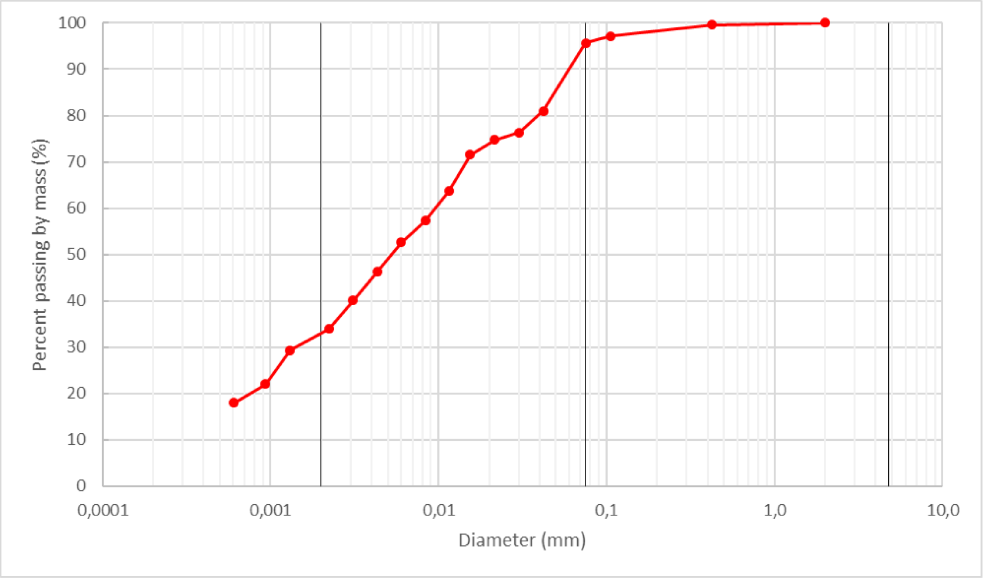

FIGURE 48 GRAIN-SIZE CURVE FROM SEDIMENTATION ANALYSIS AND WET SIEVING (S1-CR-5.30)

TABLE 8 S1-CR-5.30 FRACTIONS FROM SEDIMENTATION ANALYSIS

Coarse	%	4.4
gravel	G %	0.0
sand	S %	4.4
Fine	%	95.6
silt	M %	62.6
clay	CF %	33.0

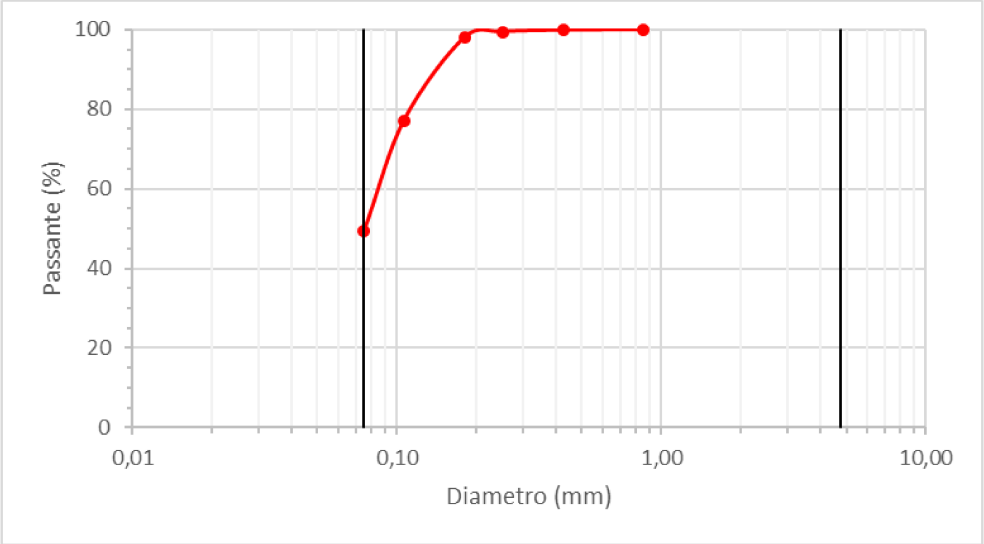

FIGURE 49 GRAIN SIZE CURVE FROM DRY SIEVING (S1-CR-6)

After the definition of the grain-size curve of each sample, another classification test is the determination of Atterberg Limits, with which the Plasticity Index (PI) can be evaluated and also, exploiting the USCS classification, the type of soil can be identified. Even in this case, several samples were tested, and the following tables report all the results obtained. Obviously, the Atterberg Limits were evaluated only for fine-grained soil samples.

After the determination of the Atterberg Limits, the Unified Soil Classification System (USCS) can be exploited in order to identify the name of the soil tested.

TABLE 9 USCS CLASSIFICATION

SAMPLE	DEPTH	ATTERBERG LIMITS			FRACTIONS						USCS
	z(m)	LL(%)	PL(%)	PI(%)	clay(%)	silt(%)	FF(%)	sand(%)	gravel(%)	CF(%)	
S1-CR-1.30	1.3				4.2	11.9	16.1	61.5	22.4	83.9	**SAND with FINES**
S1-CR-2.30	2.3	52.4	25	27.4	39.6	51.1	90.7	9.3		9.3	**FAT CLAY(CH)**
S1-CI-2.50	2.5	61.4	26.3	35.1							**FAT CLAY(CH)**
S1-CR-3.10	3.1	62.4	26.7	35.7							**FAT CLAY(CH)**
S1-CR-3.40	3.4	44.7	26.9	17.8	16.1	32.5	48.6	51.4		51.4	**SILTY SAND(SM)**
S1-CR-3.90	3.9	62	27.7	34.3	36.4	59	95.4	4.6		4.6	**FAT CLAY(CH)**
S1-CI-4.50	4.5	60.3	23.6	36.7	38.1	57.1	95.2	4.8		4.8	**FAT CLAY(CH)**
S1-CR-5.30	5.3	67.4	33.9	33.5	33	62.6	95.6	4.4		4.4	**ELASTIC SILT (MH)**
S1-CR-5.50	5.5	56.3	31.2	25.1							**ELASTIC SILT (MH)**
S1-CR-6	6			NP			49.9			50.1	**SAND with FINES**

All these laboratory tests confirm the presence of fine-grained soil deposits in the major part of the examined depth, with the exception of some sandy lenses present along the section.

One of the last characterization tests performed is the diffractometry of two samples taken one at 2.30 m depth and the other at 5.3 m depth.

Being the diffractometry a qualitative-quantitative method, thanks to this test it is possible to estimate the type and the amount of clay minerals in the samples. As can be seen in the following diagrams, the soils taken at these two different depths are characterized by the same mineral components, and even this test confirm that layers 3 and 5 can be classified as fine-grained soils.

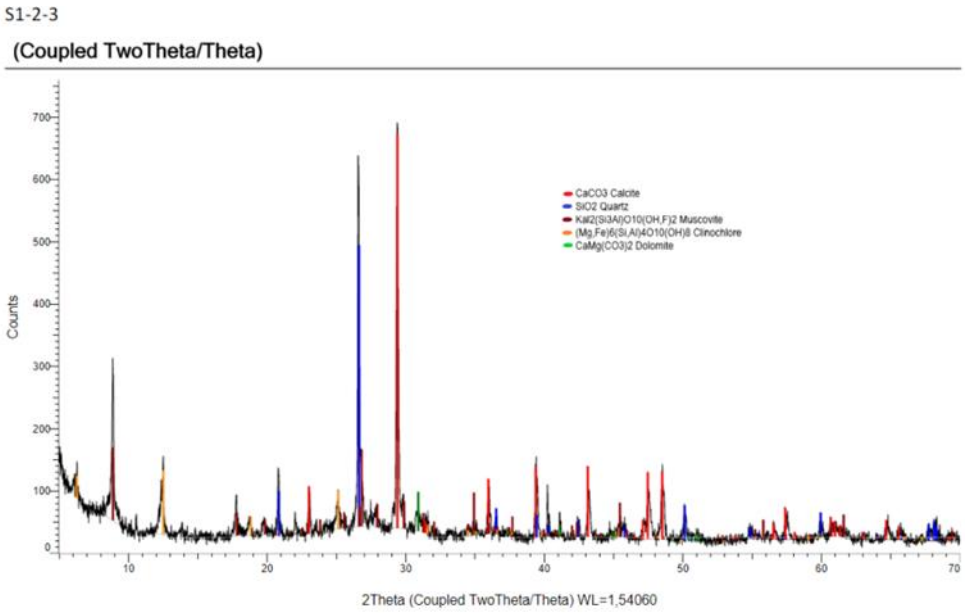

FIGURE 50 S1-2.30M X-RAY SPECTRUM

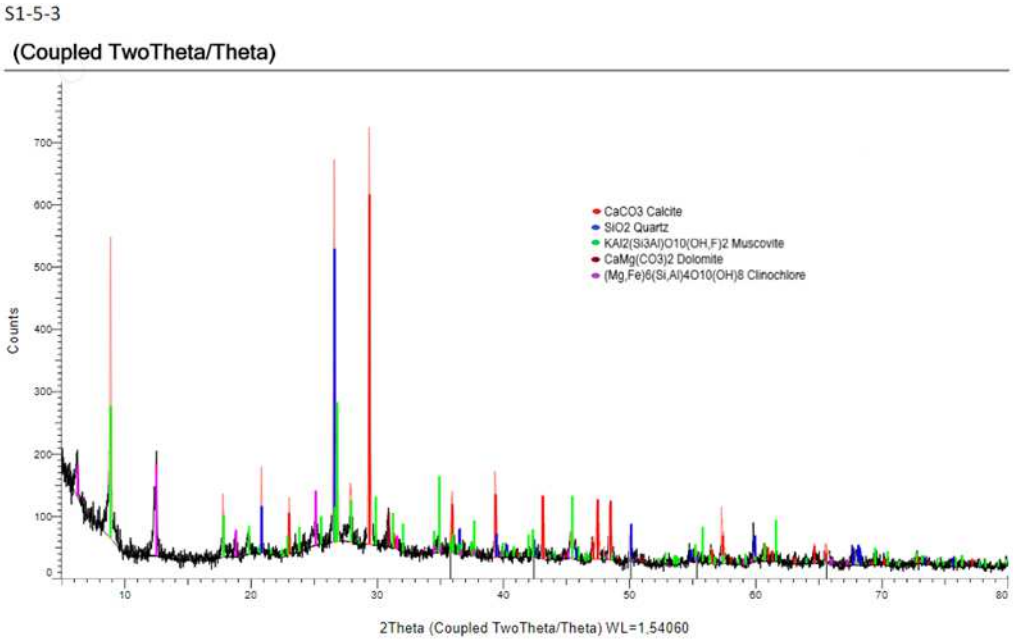

FIGURE 51 S1-5.30 X-RAY SPECTRUM

5.5 Oedometer test

The oedometer test was performed on the sample taken at 2,5m depth (taken in a layer constituted of fine-grained soil). The primary settlemets were evaluated with the Casagrande method, and the resulting compressibility curve is reported in the following graph, where three main sections can be identified: the recompression curve that is the initial part of the curve characterized by more or less zero strain, the virgin compression curve corresponding to the second section of the graph, where the slope changes abruptly, reaching a yield strength σ'_p and the specimen is more compressible, and the unloading curve which represents the swelling undergone by the specimen upon removal of the load applied.

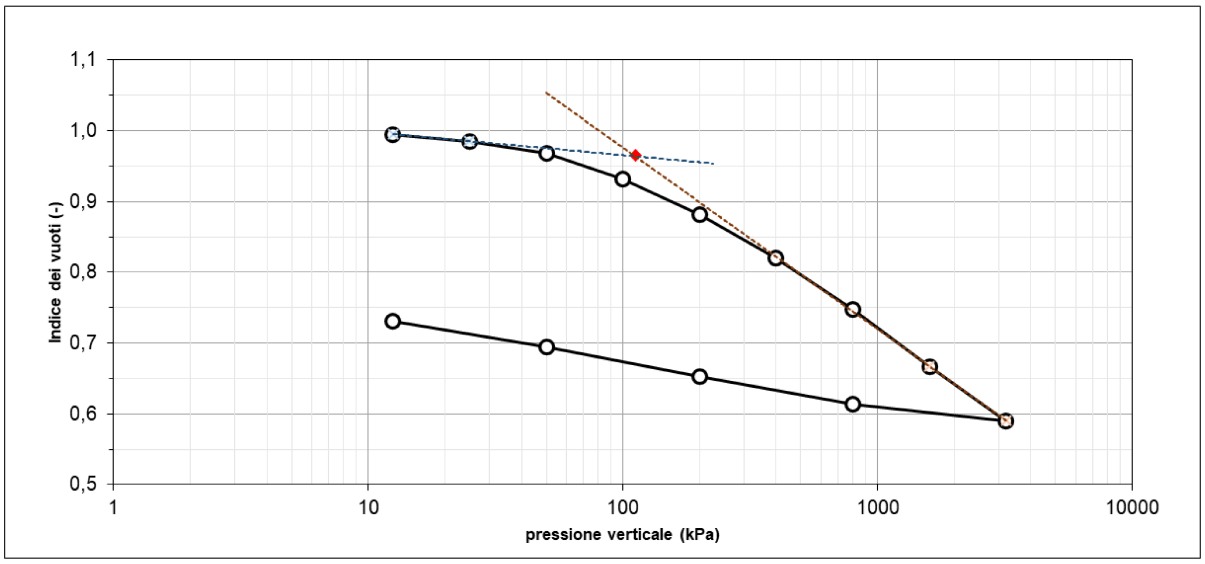

FIGURE 52 COMPRESSIBILITY CURVE

The red point plotted on the graph is the minimum preconsolidation stress σ'_p, determined with the Casagrande methodology. It can be observed that the σ'_p value is about 110 kPa, that is practically the same value of the sum of the vertical stress (considering a unit volume weight of sediments of 17.3 kN/m^3) and the maximum pressure exerted by the embankment equal to 85 kPa. Therefore, OCR results about equal to 5.5 was obtained.

5.3. Triaxial tests

For this work, triaxial tests were performed on samples taken at 2,5 m and 4,5 m depth: one unconsolidated undrained triaxial test, and one consolidated undrained triaxial test for the sample taken at 4,5 m, and one consolidated undrained triaxial tests on the 2,5 m sample.

5.3.1. UU triaxial test – sample at 4.5 m

TABLE 10 UU TRIAXIAL TEST PARAMETERS

test	n	1
D_0	mm	38
H_0	mm	76
w_0	%	41,5
$\rho 0$	Mg/m^3	1,8
$\rho d0$	Mg/m^3	1,27
$\sigma 3$	kPa	45
ε_r	%/min	0,5
q_f	kPa	38

All the resulting plots are expressed in terms of total stresses, being pore pressure not measured during the test. What can be obtained from this test is the undrained shear strength (C_u). The following graphs represent the triaxial test results.

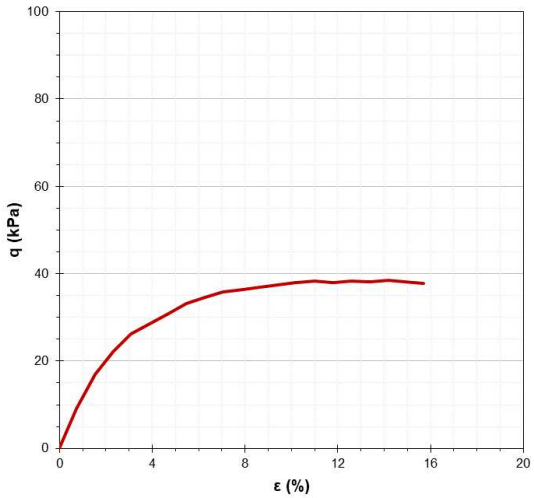

FIGURE 53 ε-Q CUVE TXUU

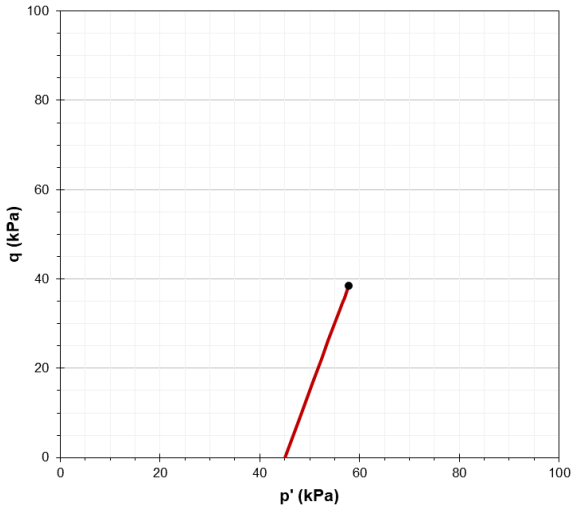

FIGURE 54 P'-Q CURVE TXUU

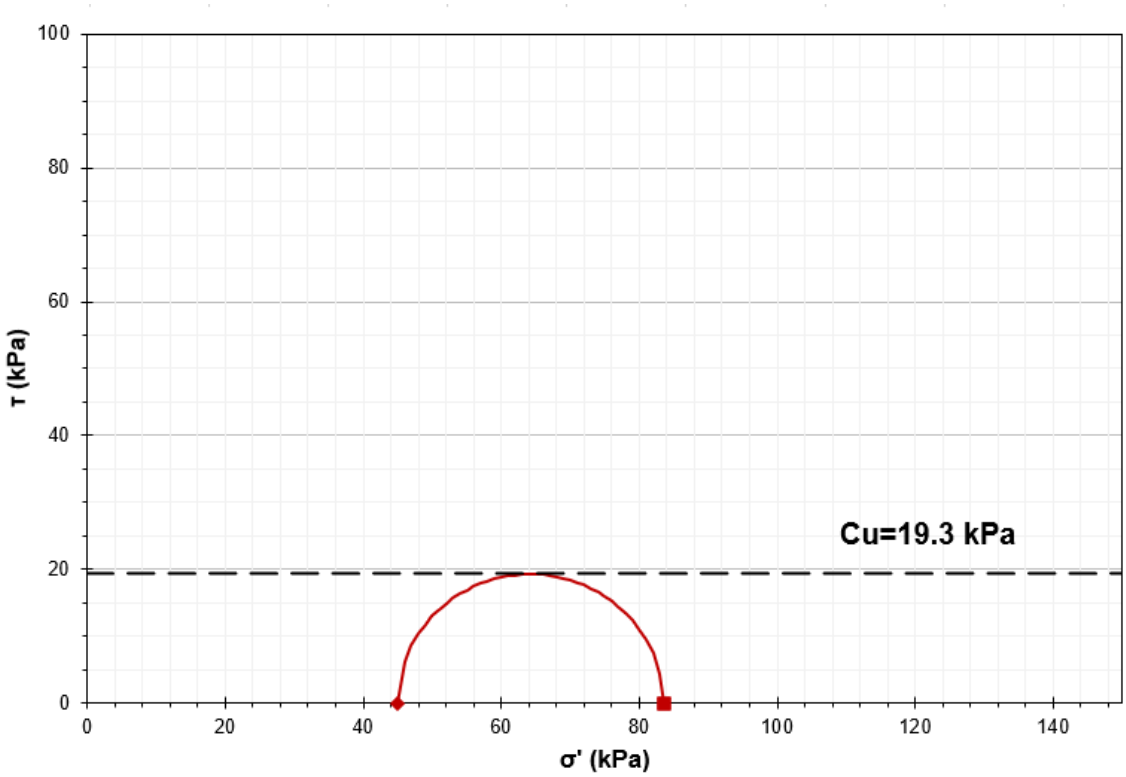

FIGURE 55 MOHR-COULOMB ENVELOPE TXUU

5.3.2. CIU triaxial test - sample at 4.5 m

TABLE 11 CIU TRIAXIAL TEST PARAMETERS (4,5M)

test	n	1	2	3
D_0	mm	38	38	38
H_0	mm	76	76	76
w_0	%	41,8	42,3	41,1
$\rho 0$	Mg/m^3	1,8	1,79	1,81
$\rho d0$	Mg/m^3	1,27	1,26	1,28
B	-	0,98	1	0,99
σ3	kPa	335	350	380
u0	kPa	300	300	300
ε_{vc}	%	2,13	2,81	4,12
w_f	%	40,2	40	37,9
ε_r	%/min	0,01	0,01	0,01
q_f	kPa	40	44	54
Δu_f	kPa	13	24	49
Eu50	Mpa	2,7	2,6	3,5

Differently from the previous case, the results are expressed in terms of effective stresses (even in total stresses is possible, but in this case only the effective stresses are considered). Stress path, and Mohr-Coulomb failure envelope are reported in the following.

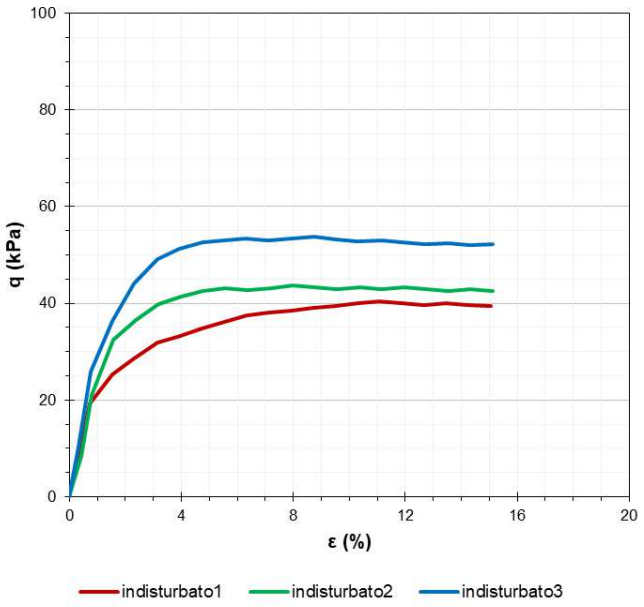

FIGURE 56 Ε-Q CURVES TXCIU (4,5M)

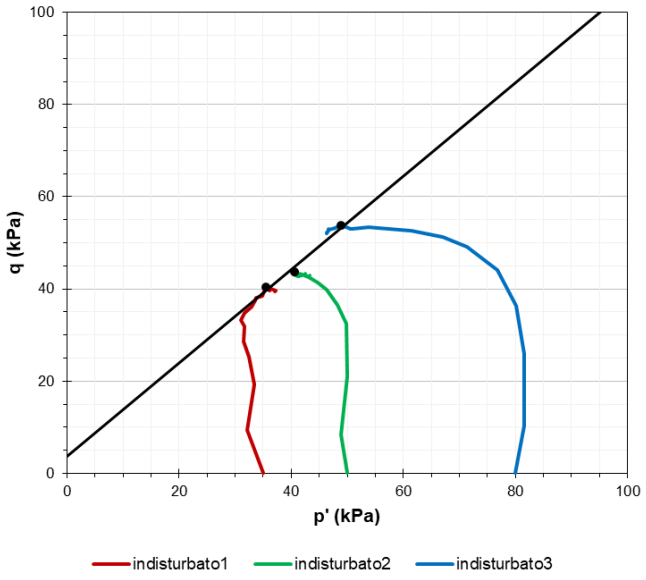

FIGURE 57 P'-Q CURVES TXCIU (4,5M)

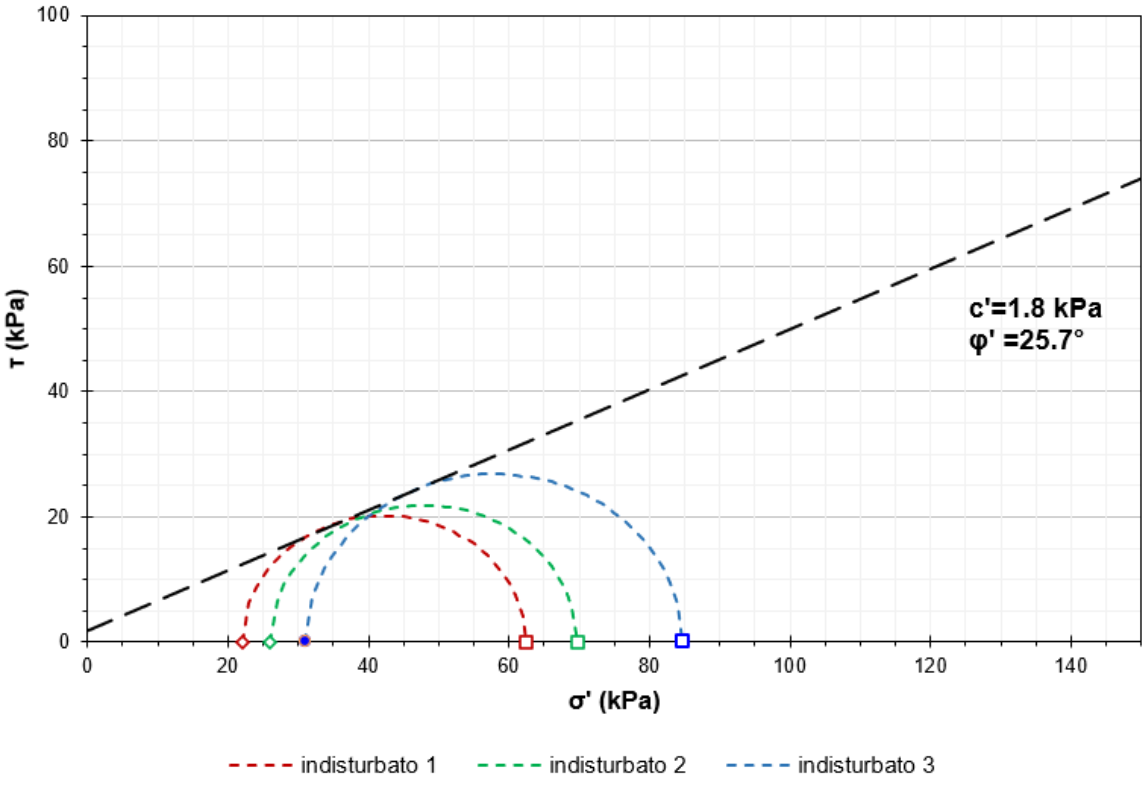

FIGURE 58 MOHR-COULOMB ENVELOPE TXCIU (4,5M)

5.3.3. CIU triaxial test - sample at 2,5 m

TABLE 12 CIU TRIAXIAL TEST PARAMETERS (2,5M)

test	n	1	2
D_0	mm	38	38
H_0	mm	76	76
w_0	%	38,2	38,1
$\rho 0$	Mg/m3	1,84	1,84
$\rho d0$	Mg/m3	1,33	1,33
B	-	0,99	0,99
σ_3	kPa	450	480
u_0	kPa	400	400
εvc	%	2,66	3,99
w_f	%	36,1	35,1
εr	%/min	0,01	0,01
q_f	kPa	61	61
Δu_f	kPa	19	45
Eu_{50}	Mpa	9,18	11,03

As the previous case, (CIU of the specimen taken at 4,5m depth), the results are expressed in terms of effective stresses (even in total stresses is possible, but in this case only the effective stresses are considered). Stress path, and Mohr-Coulomb failure envelope are reported in the following.

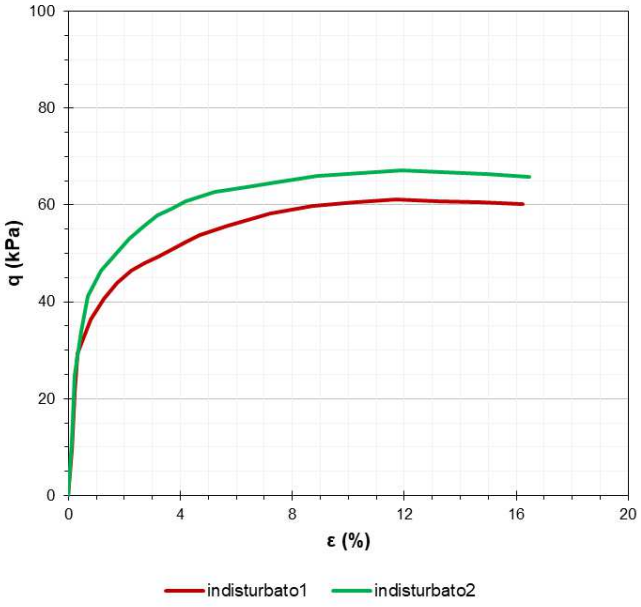

FIGURE 59 Ε-Q CURVES TXCIU (2,5M)

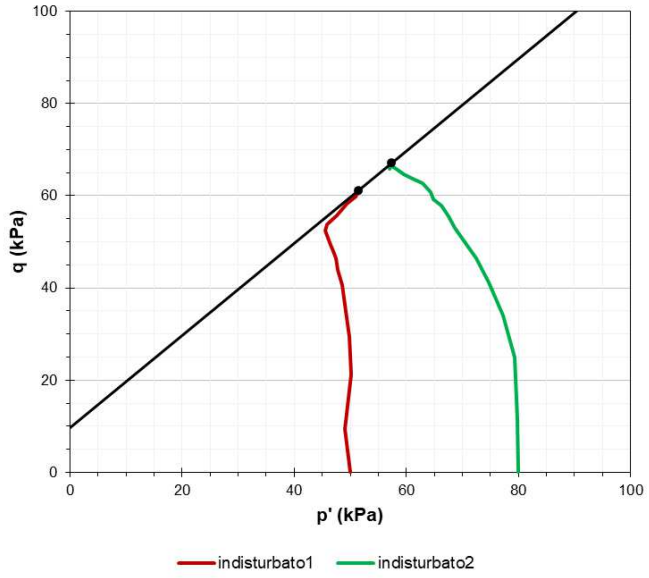

FIGURE 60 P'-Q CURVES TXCIU(2,5M)

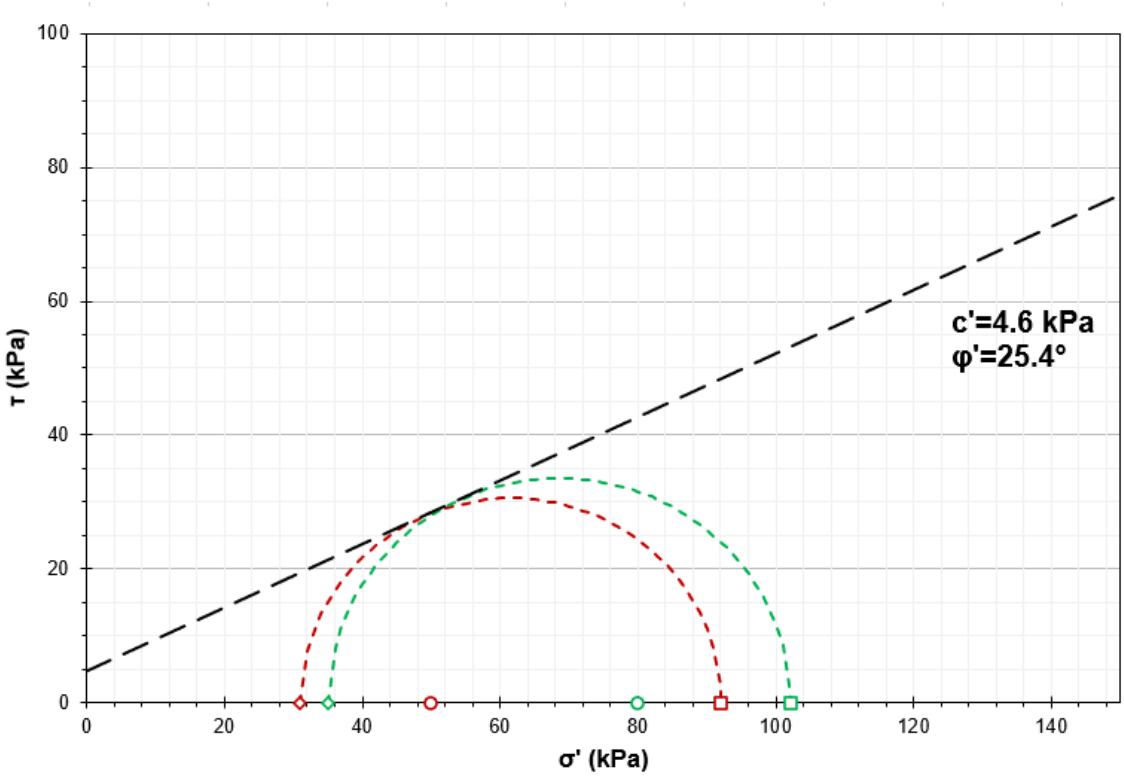

FIGURE 61 MOHR-COULOMB FAILURE ENVELOPE TXCIU(2,5M)

From these tests, the values of the undrained shear strength (C_u) at different depth and at different vertical stress applied are derived: this value will be necessary to estimate the N_k values of the vertical depth in exam.

The following table is a summary of the results obtained from the triaxial tests, in which sample depth, consolidation pressure, effective vertical stress and resulting undrained shear strength are reported. The effective vertical stress in Table 29 was obtained as detailed in § 5.4.3.

TABLE 13 RESULTS FROM TRIAXIAL TESTS

TX	depth	σ'_3	σ'_{vo}	C_u
	m	kPa	kPa	kPa
CIU	2,5	50	52,93	30,6
		80	93,08	33,6
CIU	4,5	35	32,85	20,2
		50	52,93	21,9
		80	93,08	26,9
UU	4,5	-	34,68	19,3

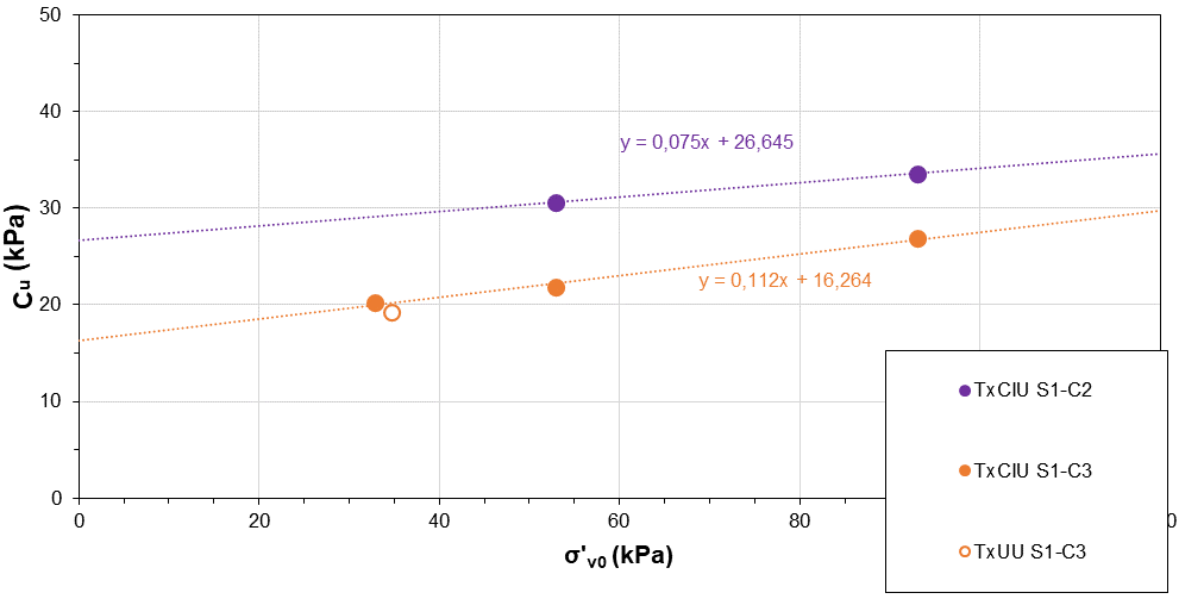

FIGURE 62 RESULTS FROM TRIAXIAL TESTS

In the above graph the obtained undrained shear strengths are reported as a function of the effective vertical stress. What can be seen, as expected, the result from the undrained unconsolidated triaxial test (white dot) agrees with that obtained with the consolidated undrained triaxial test at the same depth (blue dot).

5.4. Determination of N_k

The determination of the cone factor values (N_k) was based on the results obtained from triaxial test and these results were applied only to the stratigraphic units characterized by fine-grained soils.

5.4.1 Identification of homogeneous soil units

The identification of homogenous stratigraphic units was based on the soil classification system detailed in Cap.5.2, according to which the soil behaviour type index (I_c), can be used to discriminate between clay-like (I_c >2,6) and sandy-like (I_c <2,6). The resulting layering for the reference vertical CPTU1 is depicted in Fig. 63, where clay-like layers have been highlighted (yellow areas), as only these are of interest for the determination of N_{kt} factors.

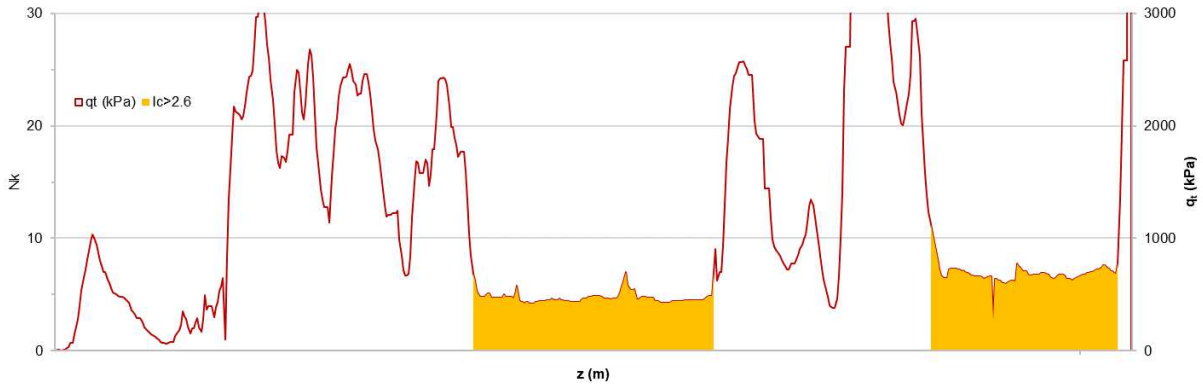

FIGURE 63 CLAY-LIKE LAYERS

As shown in Fig. 63, two clay-like units can be identified at a depth between 2.61 m and 3.6 m ("layer 3") and between 4.91 m and 5.75 m ("layer 5") respectively. It is worth to note that the fine-grained nature of these two layers was also confirmed by classification tests performed on the samples taken in the adjacent borehole; furthermore, XRD analyses evidenced that these two layers can be considered the same in terms of mineralogical composition.

5.4.2 Smoothing of the cone penetration data

Once the clay-like layers were identified, a further filtering of the q_t values was required, in order to remove anomalous spikes and to homogenize data. As suggested by Fellenius (2009), the smoothing was performed by applying the geometric average over a moving window of 50 cm length. This procedure implies that the first and latest 25 cm of the layers are inevitably disregarded from the computation, however without loss of significance.

The graph of Fig. 64 is obtained, where the blue areas indicate the values of q_t after averaging.

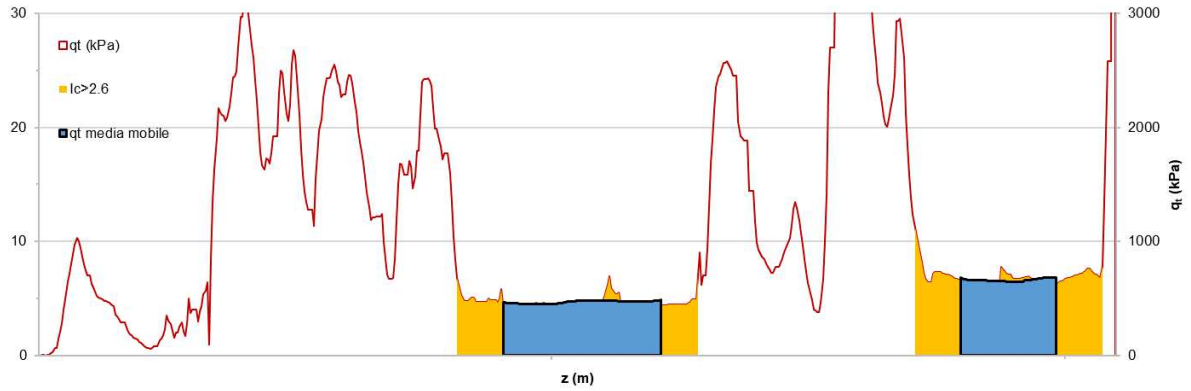

FIGURE 64 FINE-GRAINED SOIL STRATIGRAPHIC UNITS

5.4.3 Processing of triaxial tests

When searching for a relationship between cone penetration and undrained shear strength, it is crucial to state which testing method the data refer to, since the measured undrained shear strength depends on many factors such as stress history, strain rate, soil anisotropy and mode of failure (Lunne et al., 1997). In the present study, only the results of the CIU triaxial tests were used since this test proved to be adequate.

The in-situ stress state was assessed based on the field conditions (stratigraphy and depth of water table), stress history (maximum stress applied by the preloading embankment, $\Delta\sigma$), and the laboratory determined shear resistance parameters (φ'). These parameters allowed to compute the overconsolidation ratio, OCR, and the coefficient of earth pressure at rest, K_0, at each depth along the vertical of interest.

Then, the undrained shear strength values obtained from the two CIU triaxial tests described at Cap.5.3.3 were assigned to a specified vertical effective stress (i.e. depth) based on the consolidation pressure applied during the test. In particular, the consolidation stress, σ'_3, was associated to the in-situ mean effective stress, σ'_m. Then, a law of C_u as a function of σ'_{v0} was established by linear regression, to allow for the calculation of the undrained shear strength along the depth.

Namely, three relationships $C_u=C_u(\sigma'_{v0})$ were determined, based on the following approaches:

- the results from S1C2 and S1C3 were assigned to layer 3 and layer 5, respectively. The obtained relationships (Fig. 65, violet and orange lines) were considered separately.
- the results from S1C2 and S1C3 were grouped, and a single law (Fig. 65, red line) was assigned to both layers.

The first approach allowed to account for the different effect of overconsolidation induced by the preloading embankment, whereas the second one led to an easier calculation of the cone factors, with major practical significance, as discussed in the following.

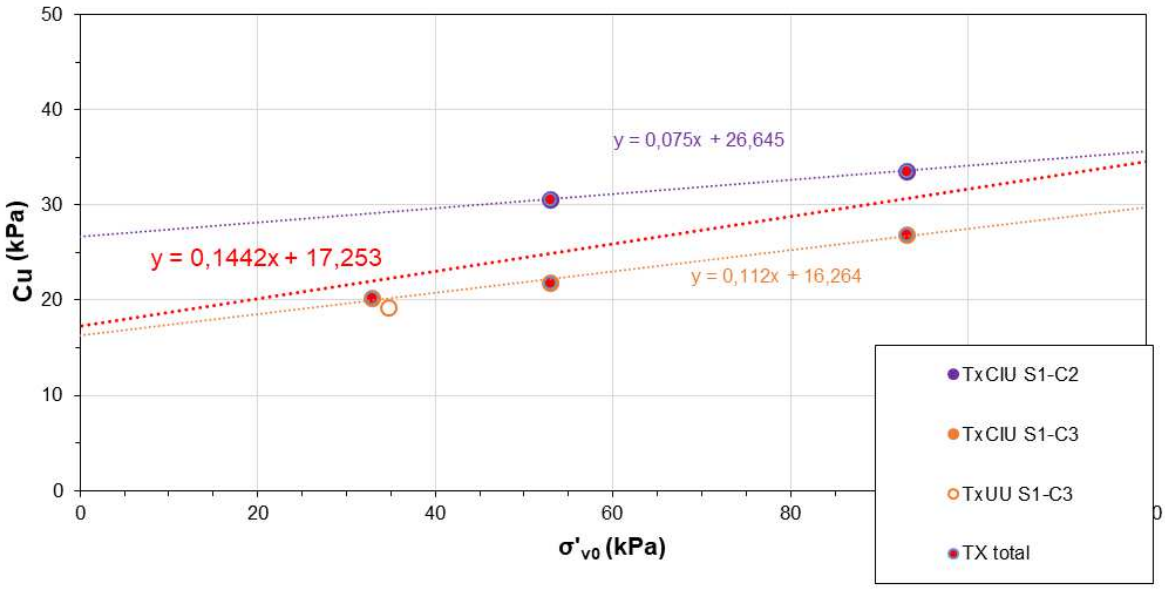

FIGURE 65 MEAN VALUES OF THE TXCIUS

5.4.4 Determination of the cone factor

Once the undrained shear strengths were evaluated, the values of N_k were estimated applying Eq. 30 to all the depth included in the blue zones of Fig 63. Since the CPTU data were available for each centimetre along the depth of the vertical section, the N_k factors were calculated for the same intervals.

As far as the first approach is concerned, two different data series were obtained: for layer 3 (between 2.61 m and 3.60 m) the N_k values are in a range of 13-16, with an average value of 15 while for layer 5 (between 4.91 and 5.75 m), the N_k values are in the range between 26 and 29 with an average value of 28. In the graph of Fig. 66, the violet dots represent the N_k factors obtained in layer 3 and the orange dots represent layer 5.

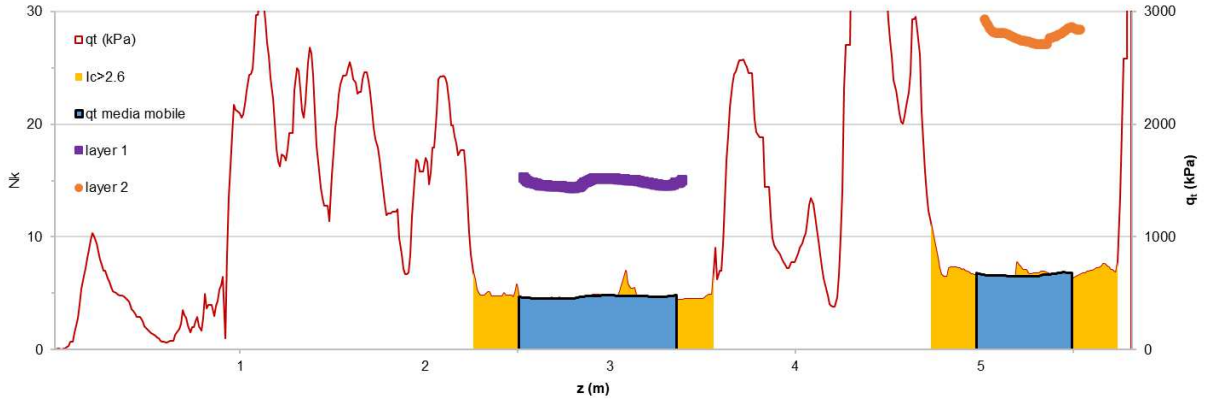

FIGURE 66 NK VALUES FROM SEPARATE TXCIU APPROACH

The main drawback of this approach lies in the large difference between the two series of N_k values, which can be reasonably ascribed to higher values of q_c, but especially to the lower values of C_u in layer 5. Indeed, the values of C_u measured on sample S1C2 are greater than those obtained from the deeper sample S1C3, possibly because the layer 5 was affected to a lesser extent by the effect of preloading.

Conversely, if one considers all the classification tests and XRD analyses performed on the samples of the vertical in question, one can assume that these two layers are practically the same material, and so a unique series of N_k factors can be computed based on Eq.30.

For this reason, a different approach was used. Taking into account all the laboratory tests performed on the samples, these two types of soil should be more or less similar (even under the mineralogical aspect, considering the results obtained from the diffractometry).

In particular, the linear regression was based on the results of both consolidated undrained triaxial tests performed, and the resulting curve can be considered as mean value of both tests, as can be seen in Fig. 65 (the red line).

The methodology applied to determine the N_k values is the same of the previous one, but in this case the results are quite different.

Specifically, what can be observed is the minor difference between the two series of data: dealing with the first section (between 2.61m and 3.6m) the N_k values are in the order of 17, while for the second section (between 4.91 m and 5.75 m) the N_k values are around 19.

The following graph shows these second method results compared to the previous ones.

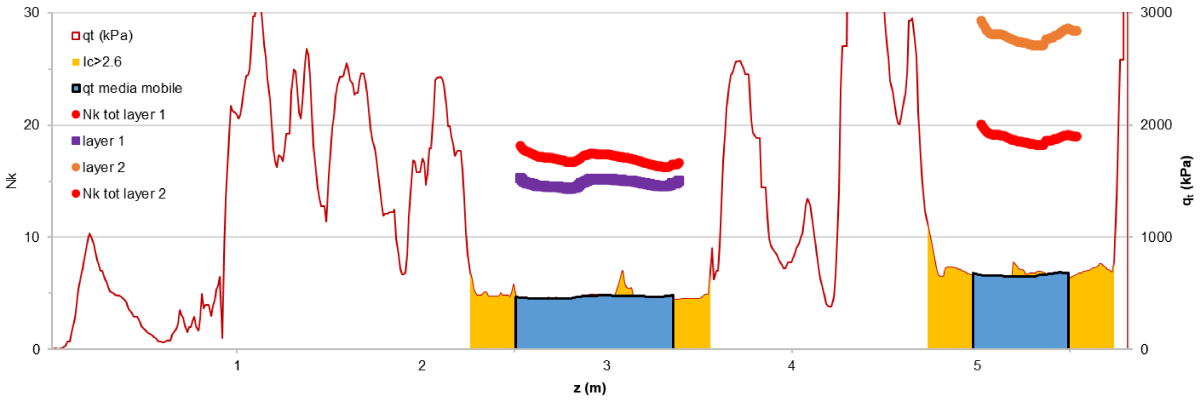

FIGURE 67 NK VALUES BASED ON BOTH TXCIU

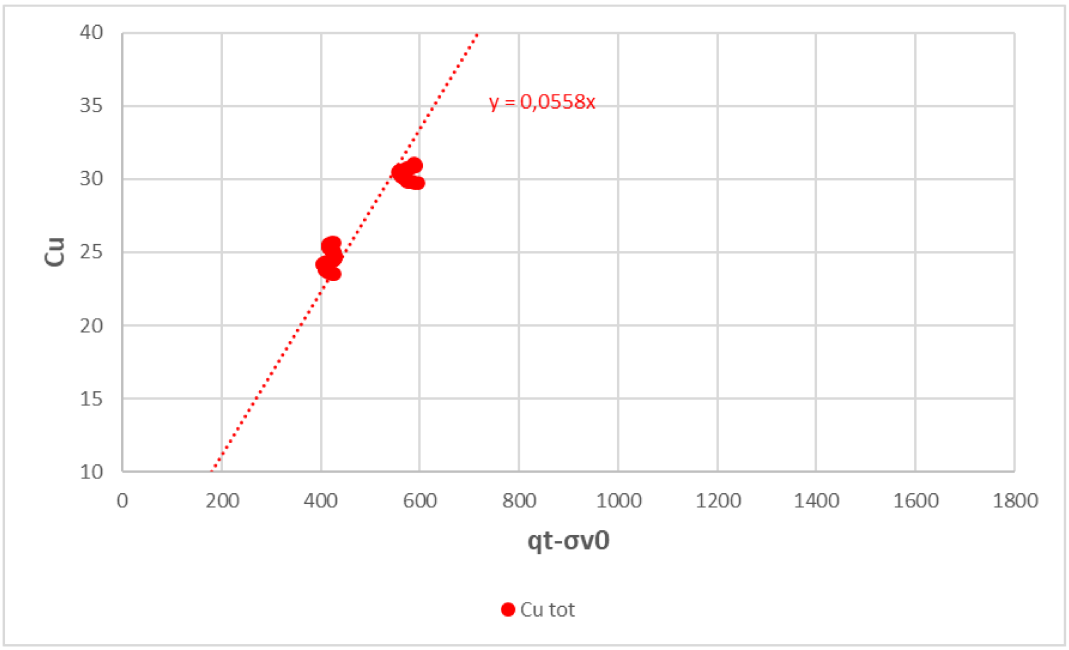

FIGURE 68 CU-QNET PLOT

Plotting the resulting curve on C_u-Q_{net} graph, where Q_{net} is the difference between the normalized cone resistance and the in -situ vertical stress, what can be evaluated is the mean value of N_k, considering it as the inverse of the angular coefficient: the result of 1/0.0558 is 17.9 that is more or less the average value of the N_k evaluated with this method.

The results obtained by this last approach agree quite well with the results which can be found in the literature as expressed in Cap. 4.1.

However, it should be stressed that the N_k values obtained are specific for the sediments having a grain size and a mineralogical composition similar to those disposed in the first sector of the Ancona CDF and subjected to a similar preloading stress. Hence, the N_k factor obtained can be used for preliminary assessment of the bearing capacity for the other sectors of the Ancona CDF but should be used with caution in other areas.

VI. CONCLUSION

The present study aimed to characterize the dredged sediments in the Confined Disposal Facility of the Ancona's Port, starting from the piezocone tests (CPTU).

One sector of the CDF, filled and consolidated by preloading and vertical drains, was investigated by CPTU tests, oedometer and triaxial tests on undisturbed samples.

The empirical correlation between the undrained shear strength and the cone resistance has been investigated with reference to the specific fine grained sediments in the CDF, on the basis of the undrained shear strength measured by consolidated-undrained triaxial tests. The aim was to determine the cone factor to be used for a rapid characterisation by CPT tests of the undrained shear strength of the sediments for design purpose after filling of the whole CDF. This indirect approach can be advantageous since it allows to avoid lot of laboratory tests on samples taken at different depths, with economical and time benefits.

Different approaches were applied, on the basis of which an average value of the cone factor N_k = 18 was obtained, even if the values resulted to vary in a large range (as found in the literature for fine-grained soils) and not depending on the plasticity of the sediments. Further research is ongoing in this regard.

It is important to stress that the empirical correlation obtained is site-specific, and it can only be applied to the examined sediments.

Figures and Tables Index

BIBLIOGRAPHY:

- ASTM D 2487-06 (2006). Standard Practice for Classification of Soils for Engineering Purpose (Unified Soil Classification System). P.A. American Society for Testing and Materials.
- ASTM D 4318-17 (2017). Standard test methods for liquid limit, plastic limit, and shrinkage limit of soils. PA: American Society for Testing and Materials.
- ASTM D2435/D2435M-11(2020) Standard Test Methods for One-Dimensional Consolidation Properties of Soils Using Incremental Loading. P.A: American Society for Testing and Materials
- ASTM D7928-21 (2021). Standard Test Method for Particle-Size Distribution (Gradation) of Fine-Grained Soils Using the Sedimentation (Hydrometer) Analysis. P.A. American Society for Testing and Materials.
- ASTM D934–22 Standard Practices for Identification of Crystalline Compounds in Water-Formed Deposits by X-Ray Diffraction. P.A.: American Society for Testing and Materials.

- Aas, G., Lacasse, S., Lunne, T., and Hoeg, K. (1986). Use of in situ tests for foundation design on clay. Proc. *of ASCE Specialty Conference In Situ '86: use of in situ test in geotechnical engineering,* Blacksburg, 1-30, ASCE

- Baligh, M. M., Azzouz, A. S., Wissa, A. Z., Martin, R. T., and Morrison, M. J. (1981). The piezocone penetrometer. Cone Penetration Testing and Experience. In Proc of the session ASCE National Convention, St. Louis, 247-63 ASCE.
- Battaglio, M., Jamiolkowski, M., Lancellotta, R., & Maniscalco, R. (1981). Piezometer probe test in cohesive deposits. In *Cone penetration testing and experience* (pp. 264-302). ASCE.

- Campanella, R. G., & PK, R. (1982). Pore pressures during cone penetration testing. Proc. 2nd European Synopsium on Penetration Testing, ESOPT II, pp. 507-512.

- Eslami, A. A., & Fellenius, B. H. (2004). CPT and CPTu data for soil profile interpretation: review of methods and a proposed new approach.

- Felici, M., Fratalocchi, E., Di Sante, M., Pasqualini, F., and Pasqualini, E. (2021). PVD-assisted consolidation of dredged sediments in a CDF: design of the test field. *Japanese Geotechnical Society Special Publication, 9*(4), 124-129.

- Felici, M., Fratalocchi, E., Domizi, J., and Pasqualini, E. (2022). Progettazione di un campo prova per il consolidamento di sedimenti in vasca di colmata. *Proc. XXVII Convegno Nazionale di Geotecnica, Reggio Calabria.*

- Fellenius, B.H. (2009). *Basics of Foundation Design*. Electronic Edition.

- Jefferies, M. G., & Davies, M. P. (1993). Use of CPTU to estimate equivalent SPT N 60. *Geotechnical Testing Journal*, *16*(4), 458-468.

- Kjekstad, O., Lunne, T., & Clausen, C. J. (1978). Comparison between in situ cone resistance and laboratory strength for overconsolidated North Sea clays. *Marine Georesources & Geotechnology*, *3*(1), 23-36.

- Konrad, J. M. (1987). Piezo-friction-cone penetrometer testing in soft clays. *Canadian Geotechnical Journal*, *24*(4), 645-652.

- La Rochelle, P., Zebdi, M., Leroueil, S., Tavenas, F., & Virely, D. (1988). Piezocone tests in sensitive clays of eastern Canada. In *International Symposium on penetration testing; ISOPT-1. 1* (pp. 831-841).

- Lunne, T., & Kleven, A. (1981). Role of CPT in North Sea foundation engineering–Session ASCE Nationali Convetion.

- Lunne, T., Christoffersen, H. P., & Tjelta, T. I. (1986). Engineering use of piezocone data in North Sea clays. *Publikasjon-Norges Geotekniske Institutt*, (163).

- Lunne, T., Eidsmoen, T., Gillespie, D., & Howland, J. D. (1986). Laboratory and field evaluation of cone penetrometers. In *Use of In Situ Tests in Geotechnical Engineering* (pp. 714-729). ASCE.

- Lunne, T., Powell, J. J., & Robertson, P. K. (1997). *Cone penetration testing in geotechnical practice*. CRC Press.

- Powell, J. J. M., & Quarterman, R. S. T. (1988). The interpretation of cone penetration tests in clays, with particular reference to rate effects. In *International Symposium on penetration testing; ISOPT-1. 1* (pp. 903-909).

- Rad, N. S., & Lunne, T. Direct correlation between piezocone test results and undrained shear strength of clay. Proc. *International Symposium on Penetration Testing*, ISOPT-1, Orlando, 2, 911-17.

- Robertson, P. K. (1990). Soil classification using the cone penetration test. *Canadian geotechnical journal, 27*(1), 151-158.

- Robertson, P. K. (2009). Interpretation of cone penetration tests—a unified approach. *Canadian geotechnical journal, 46*(11), 1337-1355.

- Robertson, P. K. (2010). Soil behaviour type from the CPT: an update. In *2nd International symposium on cone penetration testing* (Vol. 2, No. 56, p. 8). Cone Penetration Testing Organizing Committee.

- Robertson, P. K. (2016). Cone penetration test (CPT)-based soil behaviour type (SBT) classification system—an update. *Canadian Geotechnical Journal*, *53*(12), 1910-1927.

- Robertson, P. K., & Wride, B. H. (1988). Cyclic Liquifaction and the Evalution Based on the SPT and CPT. *Proceedings edited by Youd and Idriss*, 41-88.

- Robertson, P. K., Campanella, R. G., Gillespie, D., and Greig, J. (1986). Use of piezometer cone data. In *Use of in situ tests in geotechnical engineering* (pp. 1263-1280). ASCE.

- Schneider, J. A., & Moss, R. E. S. (2011). Linking cyclic stress and cyclic strain based methods for assessment of cyclic liquefaction triggering in sands. *Géotechnique Letters*, *1*(2), 31-36.

- Senneset, K. (1982). Strength and deformation parameters from cone penetration tests. In Proc. *2nd European Symposium on Penetration Testing*, ESOPT-II, Amsterdam, 2, 863-70.

- Vesic, A. S. (1972). Expansion of cavities in infinite soil mass. *Journal of Soil Mechanics & Foundations.*

- Wroth, C. P. (1984). The interpretation of in situ soil tests. *Geotechnique*, *34*(4), 449-489.

- Zhang, G., Robertson, P. K., & Brachman, R. W. (2002). Estimating liquefaction-induced ground settlements from CPT for level ground. *Canadian Geotechnical Journal*, *39*(5), 1168-1180.